UNIVERSITY OF ÇUKUROVA
INSTITUTE OF NATURAL AND APPLIED SCIENCES

MSc THESIS

Cem SAKARYA

R-PEAK DETECTION WITH WAVELET TRANSFORM

DEPARTMENT OF ELECTRICAL AND ELECTRONICS ENGINEERING

ADANA, 2013

ÇUKUROVA UNIVERSITY
INSTITUTE OF NATURAL AND APPLIED SCIENCES

R-PEAK DETECTION WITH WAVELET TRANSFORM

Cem SAKARYA

MSc THESIS

DEPARTMENT OF ELECTRICAL AND ELECTRONICS ENGINEERING

We certify that the thesis titled above was reviewed and approved for the award of degree of the Master of Science by the board of jury on 26 /01 /2013.

…….....	……..	..…….....
Asst. Prof. Dr. Sami ARICA	Assoc. Prof. Dr.Zekeriya TÜFEKÇİ	Asst. Prof. Dr. Turgay İBRİKÇİ
SUPERVISOR	MEMBER	MEMBER

This MSc Thesis is written at the Department of Institute of Natural And Applied Sciences of Çukurova University.
Registration Number:

Prof. Dr. Mustafa GÖK
Director
Institute of Natural and Applied Sciences

ABSTRACT

MSc THESIS

R-PEAK DETECTION WITH WAVELET TRANSFORM

Cem SAKARYA

UNIVERSITY OF ÇUKUROVA
INSTUTE OF NATURAL AND APPLIED SIENCES
DEPARTMENT OF ELECTRICAL AND ELECTRONICS ENGINEERING

Supervisor : Asst. Prof. Dr. Sami ARICA
Year: 2013, Pages:89
Jury : Asst. Prof. Dr. Sami ARICA
: Assoc. Prof. Dr. Zekeriya TÜFEKÇİ
: Asst. Prof. Dr. Turgay İBRİKÇİ

Electrocardiography is a technique of recording bioelectric currents generated by the heart muscles. The graphical representation of this recording is called ECG. In an ECG signal, P, Q, R, S, T, U waveforms are generated in turn at every heartbeat. The Q, R, S waves, together, forms a QRS complex. The time of its occurrence as well as its shape provide rich information about the current state of the heart and the time occurrence of the peak value of the R wave corresponds to the time occurrence of the heartbeat.

The objective of this work is to detect R-peaks in an ECG signal by using wavelet transform. A custom a multi-resolution system was designed that is suitable for detecting QRS wave. A scaling function resembling the shape of the R wave and its wavelet counterpart are designed. By employing this multi-resolution system, the approximation and detail coefficients were computed. A global threshold which is determent from the first 30 seconds of the ECG is applied to the approximation coefficients to extract the coefficients addressing the R peaks. The algorithm was also executed for common wavelets. The performance of the custom system was better than or near to the performances of the ordinary wavelets that is similar to the custom wavelet in shape. The results show that the custom wavelet can be alternative to the common wavelets in analyzing of ECG signals and for QRS detection.

Key Words: ECG, multiresolution, orthogonality, wavelet, QRS

ÖZ

YÜKSEK LİSANS TEZİ

DALGACIK DÖNÜŞÜMÜ İLE R TEPESİ BELİRLENMESİ

Cem SAKARYA

ÇUKUROVA ÜNİVERSİTESİ
FEN BİLİMLERİ ENSTİTÜSÜ
ELEKTRİK ELEKTRONİK MÜHENDİSLİĞİ ANABİLİM DALI

Danışman : Yrd. Doç. Dr. Sami ARICA
Yıl: 2013, Sayfa:89
Jüri : Yrd. Doç. Dr. Sami ARICA
: Doç. Dr. Zekeriya TÜFEKÇİ
: Yrd. Doç. Dr. Turgay İBRİKÇİ

Elektrokardiyografi kalp kasları tarafından üretilen biyoelektriksel akımların kayıt tekniği olup bu kayıtların grafiksel gösterimi EKG olarak adlandırılır. EKG de her kalp atımının karşılığı olarak sırasıyla P,Q,R,S,T,U dalga şekilleri üretilir. QRS dalgaları birlikte QRS kompleksini oluşturur. Oluşma süresinin yanı sıra şekli kalbin o andaki durumu hakkında zengin bilgiler içerir ve R dalgasının tepe değerinin oluşma süresi kalp atımının oluşma süresine tekabül eder.

Bu çalışmanın amacı, EKG sinyallerinin analizi ve sınıflandırılması özellikle QRS dalgası tespit için uygun çoklu çözünürlük sistem tasarlamaktır. R dalgasının şekline benzeyen bir ölçekleme fonksiyonu ve onun dalgacık karşılığı tasarlanmıştır. Bu çoklu çözünürlüklü sistem kullanılarak yakınlık ve detay katsayıları hesaplanmıştır. EKG'nin ilk 30 saniyelik kısmından tanımlanan yerel bir eşik seviyesi yakınlık katsayılarına R tepelerinin adresleyen katsayıları ayırmak amacıyla uygulanmıştır. Algoritma ayrıca genel dalgacıklara da uygulanmıştır. Özel sistemin performansı şekil olarak özel dalgacığa benzeyen genel dalgacıklardan daha iyi veya yakındır. Sonuçlar göstermiştir ki, özel dalgacık EKG sinyallerinin analizi ve QRS tespiti için genel dalgacıklara bir alternatif olabilir.

Anahtar Kelimeler: EKG, çoklu çözünürlük, diklik, dalgacık, QRS

ACKNOWLEDGEMENTS

I would like to express my deep gratitude to my thesis supervisor Assist. Prof. Dr. Sami ARICA for his excellent guidance, support and patience.

CONTENT **PAGE**

LIST OF TABLES **PAGE**

LIST OF FIGURES **PAGE**

LIST OF SYMBOLS AND ABBREVIATIONS

AV : Atrioventricular

CMF **:** Conjugate Mirror Filter

CWT : Continuous Wavelet Transform

DWT **:** Discrete Wavelet Transform

ECG : Electrocardiogram

FFT **:** Fast Fourier Transform

FIR **:** Finite Impulse Response

FWT : Fast Wavelet Transform

IDWT **:** Inverse Discrete Wavelet Transform

MRA **:** Multiresolution Analysis

STFT : Short-Time Fourier Transform

WT : Wavelet Transform

LP : Low Pass

HP : High Pass

$f(t)$: Scaling Function

$y\ (t)$: Wavelet Function

$\Phi(w)$: Fourier Transform of Scaling Function

$\Psi(w)$: Fourier Transform of Wavelet Function

1. INTRODUCTION

1.1. Signal Processing in Biomedical Applications

The cellular level where the voltage differences are generated is like a voltage generator and the human body produces some electrical signals in the nerves and muscles. For instance the heart produces some voltage variations that shape into a pattern (Portoles, 2009).These voltage variations show the heart's electrical activity and the recording of them is named as the Electrocardiogram (ECG). Recognition and analysis of the ECGs' are difficult because their size and form may eventually change and there can be a considerably amount of noise in the signal (Nova, 2000).

The earlier method of ECG signal analysis was based on time domain method. Time domain methods have advantage of simplicity and reproducibility. However, they are not always sufficient to study all the features of ECG signals. The frequency domain characteristics are investigated using Fourier transform. The Fourier transform is applicable to stationary signals But Fourier transform fails in some biomedical signal processing applications to provide the information regarding the exact location of frequency components in time (Gopinat et al, 1997). Because Fourier transform kernel extends in the whole time axis. So we need time frequency representation in ECG processing. One of the solutions is Short Term Fourier Transform (STFT). The signal is partitioned into equal time –segments and Fourier transform of the segments are computed. STFT has a main disadvantage in which its time frequency precision is not optimal and cannot get decent resolutions for both high and low frequencies at the same time (Karpagachelvi, 2010).

Another solution for time-frequency representation is the wavelet transform. The wavelet transform is based on the set of analyzing wavelets and each of them has its own time duration, time location and frequency band. This makes it powerful in representing and analyzing medical signals. Therefore it has been used successfully in a large number of biomedical applications. The wavelet coefficient resulting from the wavelet transform corresponds to a measurement of the ECG components in this time segment and frequency band (Saritha et al 2008).

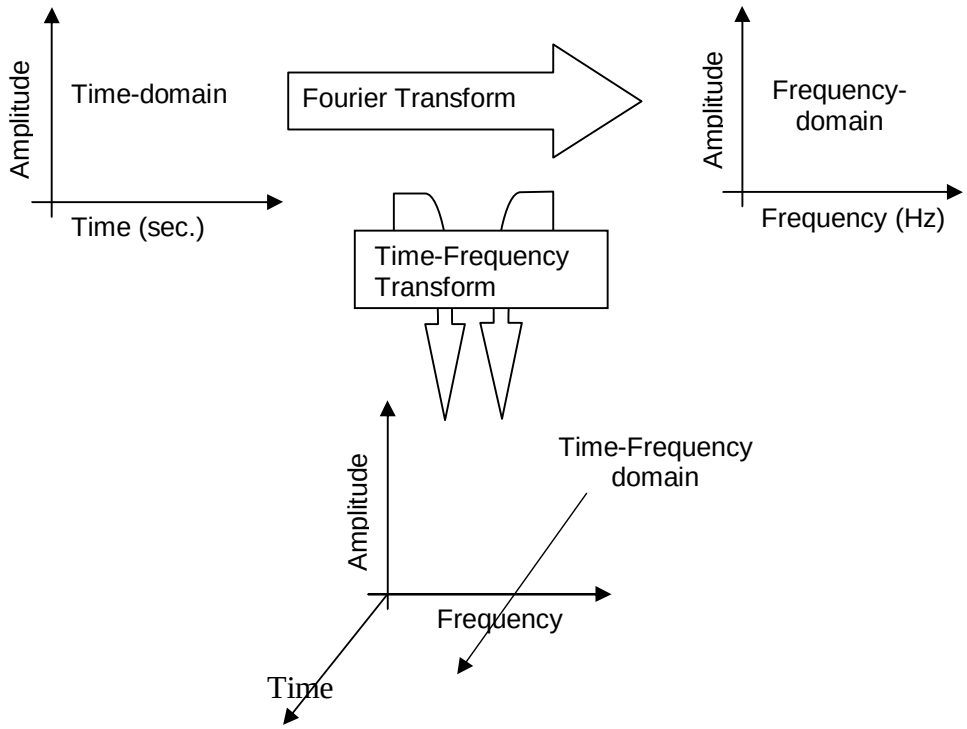

Figure 1.1.Time-frequency domain represents a combination of time-domain and frequency-domain characteristics of a signal.

Time-frequency transform provides three dimensions of a signal: the time; the frequency; and the amplitude as seen in Figure 1.1.

Wavelets are employed to analyze ECG signals for variety of; detection of the ECG characteristics, noise-filtering and compression etc..

In this thesis we develop a multi-resolution-system (scaling and wavelet function pair) to represent QRS complex efficiently in terms of small number of expansion coefficients.

For compact representation of QRS complex a function resembling the R wave is employed as the scaling. And we employ the expansion coefficients (mainly the approximation coefficients) for detecting the QRS complex; namely for locating the R wave.

This thesis is organized as follows. In the first chapter we describe ECG. Second chapter covers previous studies using multi-resolution systems in ECG analysis. The third chapter presents how a custom multi-resolution system is

generated. And we also explain the ECG detection algorithm in the third chapter. We later provide the results and finally we interpret the results and conclude.

1.2. The Data

The 'ECG' signals that we employed in this study were recorded by Arica et al. Their study was carried out at Hospital of Cukurova University, Adana, Turkey. In their study, sixteen subjects (7 male, 9 female) whose ages between 36 and 56 with a mean of 49.3 and a population standard deviation of 5 were participated and all subjects had undergone a coronary angiography and had passed the test. They recorded Lead II ECG from all 16 subjects in two consecutive 5-minute phases. The sampling frequency of the data is 1 KHz and the length of each record is 300000 samples.

1.3. Electrocardiogram (ECG)

1.3.1. ECG Recording

In ECG recording, different electrodes detect the electrical activity of the heart and ECG recorders compare these activities. This is called "a lead". Each lead gives a different view of the electrical activity of the heart, and so each ECG pattern will be different.

There are two basic types of ECG leads including *bipolar leads* and *unipolar leads*. Bipolar leads use a single positive and a single negative electrode between which electrical potentials are measured. Unipolar leads have a single positive recording electrode and a combination of the other electrodes as a composite negative electrode.

There are two types of ECG recording systems; 5-leads and 12-leads. In the 5-lead systems, there are two types of ECG recording systems; 5-leads and 12-leads. In the 5-lead systems, the electrodes are properly attached with the wires labeled 'LA' and 'RA' connected to the left and right arms, and those labeled 'LL' and 'RL'

to the left and right legs, respectively as shown in Figure 1.2-a. They coarsely form an equilateral triangle (with the heart at the center) which is called as Einthoven's triangle.

12-lead ECG system is the frequently used clinical ECG-system and it covers the 5-lead system. It consists of 12 leads which are called I, II, III, *aVR*, *aVL*, *aVF*, *V*1, *V*2, *V*3, *V*4, *V*5, *V*6. Particularly, I, II, III are three bipolar leads (Einthoven leads) . Three unipolar leads *aVR*, *aVL*, *aVF* are called Goldberger leads. Einthoven leads and Goldberger leads are positioned in the frontal plane relative to the heart. Using the axial reference and these six leads, defining the direction of an electrical vector at a given time could be simple. Additionally, Wilson leads which are denoted by *V*1 - *V*6 are unipolar chest leads and they are placed on the left side of the thorax in a nearly horizontal plane. These are shown in Figure 1.2 (Despopoulos, Silbernagl, 2001).

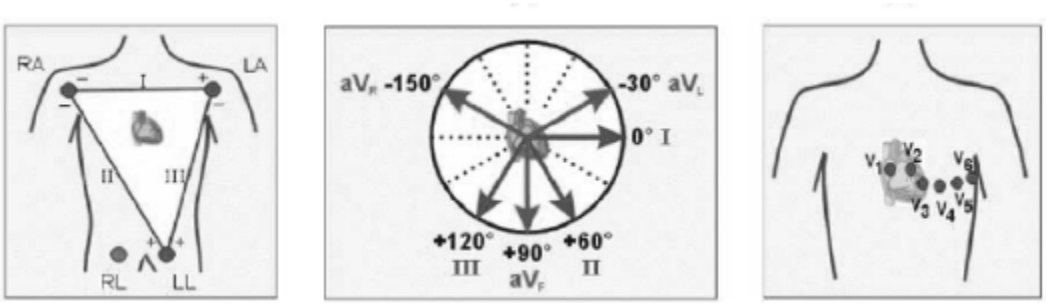

Figure 1.2. ECG leads: a) Einthoven leads; b) Goldberger leads c) Wilson leads (Despopoulos, 2001)

The Wilson leads look at the heart from the front and left side in a horizontal plane. In another word, V_1 and V_2 leads look at the right ventricle, V_3 and V_4 look at the septum between the ventricles, and V_5 and V_6 look at the anterior wall of the left ventricle (Hampton, 2003).

1.3.2. The Characteristics of ECG

The length, frequency and amplitude of ECG will be different for each person. These factors depend on the voltage, the speed and path of the impulse through the heart's electrical system (Davis, 2005).

The human ECG signals are very weak and in the mV range. The frequency range is 0.05-100Hz and most of the useful information contained in the range of 0.5-45Hz. The normal value of heart beat lies in the range of 60beats/minute to 100beats/minute (Saritha et al, 2008).

The ECGs' amplitude and intervals have useful information in clinic applications. They are defined by the characteristic points of ECG which are defined as P, QRS and T waves (and sometimes a U-wave). The letters P, Q, R, S, T were selected in the early days of ECG history, and were chosen arbitrarily. Schematic representation of an ECG signal is shown in Figure 1.3.

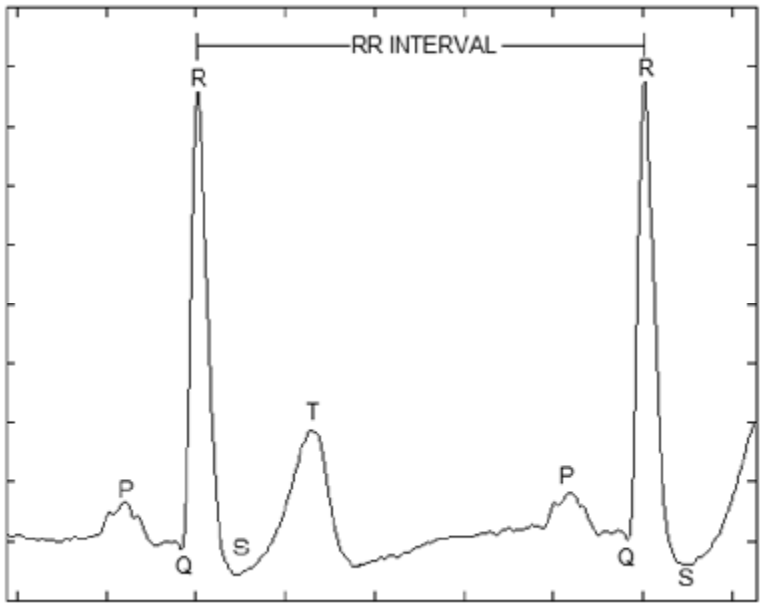

Figure 1.3.A schematic representation of the ECG and its characteristic waves.

We recall the characteristics properties of an ECG signal as below;

The P wave: The first ECG wave of the cardiac cycle is the P wave which represents activation of the atria. There is a short, relatively isoelectric segment following the P wave. The magnitude of the P wave is normally low (50-100μV) and 100ms in duration (Bronzino, 2000).

The PR Interval: The PR interval begins with the onset of the P wave and ends at the onset of the Q wave. It represents the duration of the conduction through the atria to the ventricles. Normal duration is 120ms-200ms.

The PR Segment: The PR segment begins with the endpoint of the P wave and ends at the onset of the Q wave. It represents the duration of the conduction from atrioventricular node, down the bundle of its end through the bundle branches to the muscle. There is no deflection during PR interval.

The QRS complex: The QRS complex corresponds to the period of ventricular contraction or depolarization. It is the result of ventricular depolarization through the Bundle Branches and Parkinje fibre. The QRS complex is a much larger signal than the P wave due to the volume of depolarization in the left and right sides of the heart move in opposite directions. If either side of the heart is not functioning properly, the size of the QRS complex may increase.

The ST Segment: The ST segment represents the time between the ventricular depolarization and the depolarization. The ST segment begins at the end of the QRS complex and ends at the beginning of the T wave. Normally, the ST segment measures 0.12 second or less.

The T Wave: The T wave results from the depolarization of the ventricles and is of a longer duration than the QRS complex because the ventricular depolarization happens more slowly than depolarization. Normally, the T wave has a positive deflection of about 0.5mV, although it may have a negative deflection.

The QT Interval: The QT interval begins at the onset of the Q wave and ends at the endpoint of the T wave. It represents the duration of the ventricular depolarization/depolarization cycle (Dubovik, 1999).

2. PREVIOUS STUDIES ON QRS DETECTION

A heart's condition can be determined by extracting features which include the amplitudes of the waves and the intervals between them from the ECG signal. The typical amplitude levels and durations can be determined as follows and any change in these values indicates the abnormality of the heart (Saritha et al, 2008).

Amplitude P-wave — 0.25 mV
R-wave — 1.60 mV
Q-wave — 25% R wave
T-wave — 0.1 to 0.5 mV

Duration P-R interval : 0.12 to 0.20 sec.
Q-T interval : 0.35 to 0.44 sec.
S-T interval : 0.05 to 0.15 sec.
P-wave interval : 0.11 sec.
QRS interval : 0.09 sec.

A heart rate smaller than 60 beats/min bradycardia (Slow heart) and a higher than 100 beats/min rate is called tachycardia (Fast heart). If the cycles are not evenly spaced, an arrhythmia may be indicated (Saritha et al, 2008).

Therefore it is important to detect QRS wave to identify some characteristics. The time interval between two consecutive R peaks is named as RR interval and the reciprocal of the RR interval is the heart rate. The RR sequence obtained from ECG contains information about heart rate and its variability.

There are currently a number of QRS detection algorithms available which use a variety of signal analysis methods.

Earlier works were mainly based on linear or non-linear filter or filter banks methods (Okada, 1979; Afonso, 1999). These methods use very simple models and require less computation power and are most suitable for in embedded real-time monitoring applications. The drawback is that the precision of the QRS feature extraction is limited as the processing involves only selected range of frequencies of the ECG signals.

Actually in most applications (methods) derivative methods with thresholding is employed to separate R wave from the other relatively smoother peaks.

Fraden and Neuman (1980) developed a QRS detection scheme where a threshold was calculated as a fraction of the peak value of the ECG. In 1985, Pan and Tompkins proposed an algorithm (the so-called PT method) to recognize QRS complex in which they analyzed the positions and magnitudes of sharp waves and used a special digital band pass filter (BPF) to reduce the false detection of ECG signals. In their algorithm (the so-called PT method) they first filtered the signal employing digital band pass filter. Then they differentiated the filtered signal to get information about the slope of the QRS complex, squared it to amplify the output of derivation stage and then computed integral of each moving window to quantify QRS and non-QRS. A threshold level for every two second- signal is determined. And thresholding is done for both differentiated and squared-integrated signal to improve the reliability. Also in 1997 Ruha et al filtered the ECG signal with a matched filter to suppress the P and T waves and noise first, then the QRS complexes were enhanced by passing through a nonlinear transformation, at last, the QRS complexes' location were determined.

Li et al (1995) who proposed a method based on finding the modulus maxima larger than a threshold obtained from the pre-processing of preselected initial beats. In Li et al's method, the threshold is updated during the analysis to obtain a better performance. This method has a post-processing phase in which redundant R waves or noise peaks are removed. The algorithm achieves a good performance with a reported sensitivity of 99.90% and positive prediction value of 99.94% when tested on the MIT/BIH database.

Wavelet based QRS detection are also widely examined (1995;Li et al.,1993; Sahambi et al.,1997; Mahmoodabadi et al., 2005; Sasikala et al 2010; Bsoul et al., 2009). With the wavelet based analysis, each QRS complex corresponds to a couple of maximum and minimum in wavelet transform. Using different scales in the analysis in time-and frequency-domain, the signals are divided into different response clusters which represent different frequency components of the ECG.

Kozakevicius et al (1988) utilized orthogonal wavelets to filter and analyze ECG signals. They used compactly supported wavelets associated to the statistical Stein's Unbiased Risk Estimator in order to obtain an adaptive thresholding strategy to filter ECG signals and then they analyzed the filtered signals by using the Haar wavelet transform in order to detect the positions of the occurrence of the QRS complex during the period of analysis.

Kadambe et.al (1999) described a QRS complex detector based on the dyadic wavelet transform (DWT) which was robust to time-varying QRS complex morphology and to noise. They designed a spline wavelet that was suitable for QRS detection. The scales of this wavelet were chosen based on the spectral characteristics of the ECG signal. They performed their QRS detection algorithm upon American Heart Association (AHA) data base and the algorithm have different performances with an error of 0.2% - 15.4% for different ECG records. Szilagyi et al. (2001) constructed a QRS complex detection algorithm that could be applied in various on-line ECG processing systems. They first filtered the signal with wavelet transform filtering to eliminate the low pass and high pass frequency components. Then by wavelet transform they obtained a few maxima and minima in each period of the transformed signal and detected the extreme values. The peaks which came before a long ascent and followed by a long descent of the signal are offered R peaks. They tested the algorithm to MIT-BIH database and had detection ration between 98.9% and 100%.

Legarreta et al (2005) have extended the work of Li et al and Kadambe et al, utilizing the continuous wavelet transform. Their CWT-based algorithm affords high time–frequency resolution which provides a better definition of the QRS modulus maxima curves. This allows them to follow QRS wave across scales in noisy signals, and better define the spectral region corresponding to the QRS maxima peak. They tested the algorithm using patient signals recorded in the Coronary Care Unit of the Royal Infirmary of Edinburgh with a positive predictive value of 99.73% and with the MIT/BIH database obtaining a positive predictive value of 99.68%.

In 2006, S.A.Choukari et al used second level wavelet coefficients for detecting QRS complex and fourth and fifth level coefficients of decomposition for

detecting P and T waves and by combining of them they constructed the denoised ECG signal. They compared the performance of their algorithm with db5, db10, coif5, sym6, sym8, biorth5.5 by calculating MSE and SNR. In 2007, M.Kania et al studied the importance of the proper selection of mother wavelet with appropriate number of decomposition levels for reducing the noise from the ECG signal. The authors claimed that they obtained good quality signal for the wavelet db1 at first and fourth level of decomposition and sym3 for fourth level of decomposition.

In 2008, Rizzi et al proposed and implemented an algorithm called R-point detector based adaptation of fast parallelized wavelet transforms for the detection of R-wave in the presence of different types of noises. The algorithm gave high degree of noise immunity and predictivity.

In general researchers used some known wavelet functions to detect QRS complexes. Ktata et al (2006) used Daubechies 1 wavelet to produce an algorithm for detecting not only QRS complex but P wave and R wave. They decomposes the ECG signal into five levels by using continuous wavelet, to obtain the scalogram of ECG and the detection of R peaks is reached from level number one but the detection of T wave and P wave is reached from level four and five. They used a rectangular window centered in the maxima detected for each wave to make a truncation and then mark-up the ECG signal by maximum detected. Daqrouq et al (2008) used Symlet as a wavelet function. Their detector was based on using the CWT with sym8 and scale 2^3. They calculated the wavelet approximation coefficients with applying the known Mallat's algorithm and then they computed the square of coefficients to specify a threshold level for detecting the maximum in every window, which indicated the R peaks. They also computed the R-R interval and heart rate. The average rate of QRS detector achieved is about 99.75. In 2008, Rizzi et al proposed and implemented an algorithm called R-point detector based on adaptation of fast parallelized wavelet transforms for the detection of R-wave in the presence of different types of noises. They selected the bior 3.3 wavelet as a mother wavelet because of its similar shape to a QRS complex. They applied soft thresholding technique into dyadic scales and decomposed the ECG signal. They evaluated the algorithm to MIT-BIH Noise Stress Test Database with a 99.6% detection success.

Elgendi et al (2010) used Coiflet as a wavelet function. Their algorithm using an adaptive threshold based on an approximation of signal-to-noise ratio was developed to detect QRS complexes in arrhythmia ECG Signals that suffer from non-stationary effects, low Signal-to-Noise ratio, negative QRS polarities, low QRS amplitudes and ventricular ectopic. They investigated which of the Coiflet wavelets achieves the best detection rates. Their method was tested on MIT/BIH Arrhythmia Database with 98.2% average success of correctly detecting beats. Karpagachelvi et al (2010) developed an ECG feature extraction system based on multi resolution WT. They first employed Haar wavelet to denoise the ECG signal by Discrete Wavelet Transform and detected the R peaks which are over the threshold level. They examined the performance of the R-peaks detector by testing their algorithm on the standardized MIT_BIH database.

In 2007 Kumari et al constructed their wavelets, used them for QRS detection, reconstructed the ECG signal and compared the performance with standard wavelets like dB4 and bior 4.4. They construct two filters that meet certain requirements to enable perfect reconstruction and to yield an orthogonal underlying wavelet basis.

There are also methods other than derivation and wavelet techniques and is summarized in the following.

Martinez et al (2004) utilize an algorithm to detect QRS based on the fact that QRS complexes have more energy and higher amplitude and maxima lines over a longer frequency interval, and P and T waves have less energy and lower amplitude and maxima lines over a shorter frequency interval. The QRS components also have a different shape from the rest of the ECG waveform; - a difference that enables simple QRS detection.

Chawla et al (2006) suggested a model for ECG using Principle component analysis as a signal expansion method. They created eigenvectors which form a new orthogonal basis finding various segments of an ECG waveform and they used Fast Fourier Transform for the results and extracted the QRS complex portion and excluded P-wave and T-wave.

Hilbert transform method also was used. Zhou et al (1988) used Hilbert transform first time. In 2000 Benitez et al proposed an algorithm for detecting QRS using Hilbert Transform. They used a moving 1024 points rectangular window to subdivide the signal, differentiated them and performed the Hilbert Transform. They applied an adaptive threshold level to Hilbert sequence to detect the R peaks. When two detected R peaks are very close each other (less than 200 ms), only one of them is selected as the R peak. They tested their algorithm upon MIT-BIH Arrhythmia database with QRS detection error rate of 0.36%. Oliveria and Cortez (2004) used Hilbert transform pairs of wavelet bases in order to develop pass band filter between 5-40Hz to emphasize the R wave peaks and they determined the RR intervals from that signal.

Neural network applications were also used for QRS detection. Viyaja et al (1997) used predictive neural network based technique. They trained the network for two classes; QRS and non-QRS using the back propagation algorithm predict the QRS from the ECG signal. Abibullaev & Hee Don Seo (2009) presented a method for detection and classification of QRS complexes in ECG signals using continuous wavelets and neural networks. They analyzed ECG by using dB5, sym4, bior 1.3 and bior 6.8 wavelets. They employed these wavelets as the mother wavelet, applied continuous wavelet transform decomposition, determined an adaptive threshold level and handled few wavelet coefficients after thresholding. Then they used three layer feed forward networks with back propagation learning algorithm. They evaluated their algorithm using arrhythmic ECG data from the American Heart Association database with an average accuracy of 95.78%.

Xue et al (1992), Cohen et al(1995), Tan et al (2000) also studied neural Networks algorithms.

3. MATERIAL AND METHODS

3.1. Wavelets

The *wavelet transform* is probably the most recent solution to overcome the shortcomings of the Fourier transform that mentioned in Section 1.1. In wavelet analysis, a window is shifted along the signal and for every position of the window and some wavelet coefficients are calculated. Then this process is repeated many times with a slightly shorter (or longer) window for every new cycle. In the end the result is the collection of time-frequency representations of a signal with different resolutions (Howard, 2005). It is designed to give good time resolution and poor frequency resolution at high frequencies and good frequency resolution and poor time resolution at low frequencies. This approach makes sense especially when the signal has high frequency components for short durations and low frequency components for long durations. This is mostly seen biological signals, mainly EEG, EMG and ECG signals.

3.1.1. The Continuous Wavelet Transform

Let $y(t) \in L^2(R)$ is a continuous-time mother wavelet function and the set of functions, obtained by shifting and scaling the mother wavelets

$$y_{a,b} = \frac{1}{\sqrt{a}} y\left(\frac{t-b}{a}\right)$$

are orthonormal wavelet basis in the $L^2(R)$. That is $\int_{-\infty}^{\infty} y_{a,b}(t)\, y^{*}_{a',b'}(t)\, dt = d(a-a')\, d(b-b')$. In the wavelet, a and b variables are real and the integral value indicate the closeness of the signal to a particular basis function. Dividing $y_{a,b}(t)$ by $\sqrt{a}$ insures the unity in the L^2 norm of the set

$\{y_{b,a}(t)\}$ (Mertins, 1999) (Grossmann, 1984). The main disadvantages of the CWT are computational complexity and redundancy.

The mother wavelet has to satisfy the following properties. (Addison, 2002);

1. A wavelet must have finite energy

$$E = \int |y(t)|^2 dt < \infty$$

2. $y(t)$ integrates over time to zero (It's Fourier transform $\Psi(w)$ equals to zero at $w = 0$) (Mertins,1999)

$$\Psi(w=0) = \int_{-\infty}^{\infty} y(t)dt = 0$$

The correlation between the signal and the wavelet is defined as the integral of their product.

3.1.2. The Discrete Wavelet Transform

The discrete wavelet transform (DWT) is obtained in general by sampling the corresponding continuous wavelet transform (Teolis, 1998). To discretize the CWT, an analyzing wavelet function that generates an orthonormal (or bi-orthonormal) basis for the space of interest is required. There are many possible discretization of the CWT, but the most common DWT uses a dyadic sampling lattice, in which $a = 2^{-j}$ and $b = 2^{-j}k$. Figure 3.1 shows the time-scale cells corresponding to dyadic sampling (Mallat, 1989).

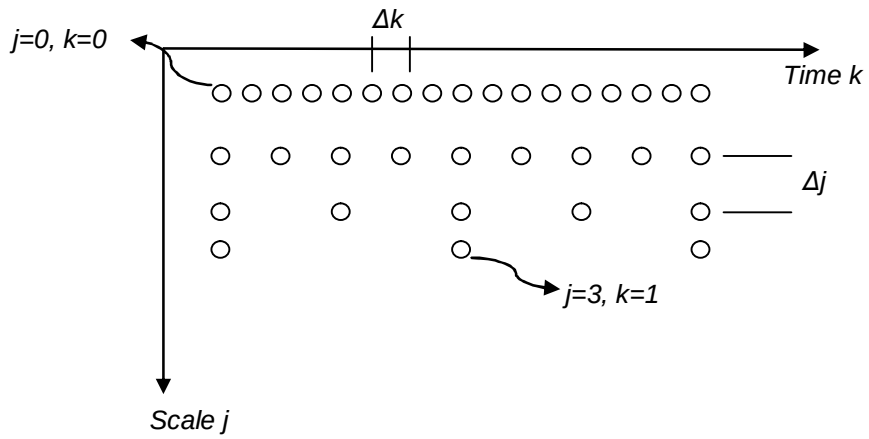

Figure 3.1. Time-scale cells corresponding to dyadic sampling (Mallat, 1989).

The discrete wavelet which is generated by dyadic sampling from the continuous wavelet transform is given by

$$y_{j,k} = 2^{j/2} y\,(2^j t - k) \tag{3.1.}$$

$y_{j,k}$ is known as wavelet basis and we employ linear combinations of basis functions which localized both in time and frequency to construct a signal function *(f(t))* is a linear combinations of basis functions. So we can express a signal function as; (Ganesan, 2004);

$$f(t) = \sum_{j=-\infty}^{\infty} \sum_{k=-\infty}^{\infty} b_{j,k} y_{j,k}(t) \tag{3.2.}$$

where

$$b_{j,k} = \int_{-\infty}^{\infty} f(t) y_{j,k}(t)\,dt \tag{3.3.}$$

are the time-scale coefficients as in Figure 3.1.

3.2. Multi-Resolution Analysis

Wavelet transform leads to a signal decomposition technique named as multiresolution analysis (MRA) which analyzes the signal at different frequencies with different resolutions.

The idea is; there is a scaling transformation which moves in discrete steps, up and down an associated scale of subspaces. One of the resolution scales refers to "coarse," and the other to "fine". When we compare two subspaces, we can see that the space of the coarse scale is contained in that of the fine resolution (Jorgensen, 2006).

The WT is based on the scaling function. The scaling function is a continuous, square integrable and, in general, real-valued function and is not equal to zero, but is usually normalized to unity. The basic scaling function $f(t)$ is shifted by discrete translation factors as;

$$f_{j,k}(t) = 2^{j/2} f\left(2^{j/2} t - k\right) \tag{3.4.}$$

where j and k dilation (scale) and translation indices respectively and can take on only integer values. Dilation and time parameters determine frequency and the time resolution of the WT. As the small values of the dilation parameter providing good time localization and poor frequency resolution, the large values of the dilation parameter provides good frequency resolution and poor time resolution. Translation parameter produces the time delay.

A function ($f(t)$) in the whole space has a piece in each subspace. Those pieces contain more and more of the full information in $f(t)$. The piece in V_j is $f_j(t)$. One requirement on the sequence of subspaces is completeness:

$$f_j(t) \to f(t) \quad \text{as} \quad j \to \infty .$$

Let W_0 be the space spanned by the orthonormal set of bases $\{y(t-k), k \in \mathrm{N}\}$. Space W_0 is orthogonal to the space W_1. Then spaces spanned by wavelet function bases are orthogonal among themselves. Thus, $\ldots W_{-1} \perp W_0 \perp W_1 \perp W_2 \perp \ldots$

Any signal in V_1 space could be expressed in terms of bases of V_0 and W_0 space. If we combine the bases of V_0 and W_0 space, we can define any signal in V_1 space as:

$$V_1 = V_0 \oplus W_0$$

W_0 is the complementary of V_0 while V_0 is subset of V_1. So V_0 and W_0 spaces are complementary. We call two spaces that satisfy this property orthogonal and use $V_j \perp W_j$ to denote V_j is orthogonal to W_j. Their bases together can represent any signal in the next "higher" or finer space of V_1 (Soman, 2004). V_j denotes subspaces corresponding to scaling basis (approximations) and W_j denotes subspaces corresponding to wavelet basis (details).

The part of the signal at resolution j and space V_j is the approximation of the signal at this resolution;

$$a_j(t) = \sum_{k=-\infty}^{\infty} a_k f_{j,k}(t) \qquad (3.5.)$$

and the part of the signal at resolution j and space W_j is the detail of the signal at this resolution;

$$d_j(t) = \sum_{k=-\infty}^{\infty} b_k y_{j,k}(t) \qquad (3.6.)$$

The signal at the resolution j is then

$$f_j(t) = a_j(t) + d_j(t) \qquad (3.7.)$$

The relationship between scaling and wavelet function spaces is shown in Figure 3.2. Spaces spanned by scaling function bases are nested. Each V_j is contained in the next subspace V_{j+1}.

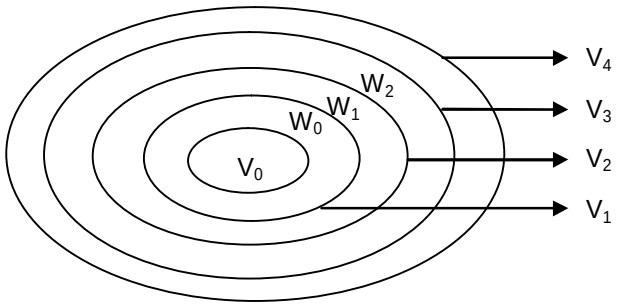

Figure 3.2. Nested vector spaces spanned by scaling and wavelet basis.

We can represent the wavelet decomposition process schematically in Figure 3.3.

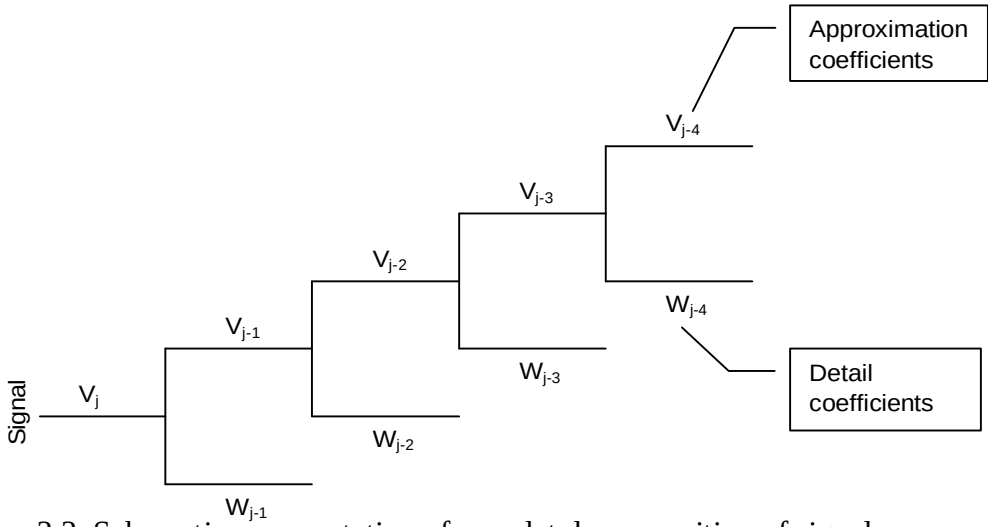

Figure 3.3. Schematic representation of wavelet decomposition of signals

Below the properties multiresolution analysis is summarized.

A multiresolution analysis or system should have the following properties or conditions. A *multiresolution analysis* of L^2(R) is a sequence $\{V_j\}\ j \in Z$ of subspaces of L^2(R). The V_j's model spaces of signals having resolution at most 2^j.

i.) Every signal lies in some V_j,

ii.) No signal, except the null signal, belongs to all V_j (Jorgensen, 2006).

iii.) The V_j are nested within one another.

iv.) The intersection of the V_j is the signal of zero norm (zero almost everywhere), which we write $\mathbf{I}_j V_j = \{0\}$

v.) The union of the V_j is dense in L^2(R): $\overline{\mathbf{U}_j V_j} = L^2(R)$

vi.) V_j is closed under time shifts $t \to t - k2^j$ and $f(t) \in V_0$ is equivalent to $f(2^j t) \in V_j$.

vii.) Elements of the spaces are dyadically scaled versions of one another:

viii.) $f(t) \in V_0 \Rightarrow f(t-k) \in V_0$

ix.) There exists a function $f(t) \in V_j$ such that the set $\{j(t-k), k \in Z\}$ forms a basis of V_o (Mallat, 1989)

x.) $f(t) \in W_0 \leftrightarrow f(2^j) \in W_j$

xi.) Shift invariance for W_j's: $f\left(2^j\right) \in W_j \leftrightarrow f(2^j - k) \in W_j$

xii.) Orthonormality between wavelet spaces: $W_j \perp W_k, j \neq k$

3.2.1. Two-Scale Relation

Let $f(t)$ translates with integer step span the subspace V_0. At the next finer resolution the subspace V_1 is spanned by the set $\{f(2t-k)\}$. The scaling function at

resolution index $j=0$ can be decomposed as a linear combination of the scaling functions at the higher resolution level $j=1$, as:

$$f(t)=\sum_{k} p(k)f(2t-k) \tag{3.8.}$$

where the discrete decomposition coefficient sequence $p(k)$ is called the inter-scale coefficients and it is a discrete low-pass filter. This equation is also called as dilation equation. This decomposition may be considered as the projection of the basis function $f(t)\in V_o$ onto the finer resolution subspace V_1. The sequence $p(k)$ governs the structure of the scaling function. We can also expand $y(t)$ onto the scaling function basis $f(2t-k)$ in the finer resolution subspace V_1 as:

$$y(t)=\sum_{k} q(k)f(2t-k) \tag{3.9.}$$

where the sequence $q(k)$ is the inter-scale coefficients and it is a discrete high-pass filter. This equation is known as two-scale equation and it defines the relations between $f(t)$ and $y(t)$ and the discrete sequences of the $p(k)$ and $q(k)$ (Sheng, 2000).

3.3. Properties of Orthogonal Multiresolution System and Orthogonalization

On the wavelet transform, orthogonal wavelet functions will have no overlap with each other (zero correlation), while nonorthogonal wavelets will have some overlap (nonzero correlation). A signal could be transformed to wavelet space and back with no loss of information by using an orthogonal wavelet. Because of the overlap, nonorthogonal wavelet functions add artificial energy to the signal and so it requires renormalizing the information for conserving. If an error presents in the

initial data, it will not grow under the transformation. When we want to preserve the energy of the signal in transform domain and to reconstruct a signal from the coefficients, orthogonality should be considered an important property (Dinh et al, 2001). Consider the scaling function $f(t)$ and the wavelet function $y(t)$ of an orthogonal multi-resolution system. The following characteristics of the scaling and wavelet function can easily be deduced from the properties of multi-resolution spaces mentioned previously.

$$\int_{-\infty}^{\infty} f\left(2^j t\right) f\left(2^j t-k\right) dt = d(k) \tag{3.10.}$$

$$\int_{-\infty}^{\infty} f\left(2^j t\right) y\left(2^j t-k\right) dt = 0 \tag{3.11.}$$

$$\int_{-\infty}^{\infty} y\left(2^j t\right) y\left(2^{j+m} t-k\right) dt = d(m) d(k) \tag{3.12.}$$

At scale $j=0$ we rewrite orthogonality of the scaling function to its translates in Equation (3.10.).

$$\int_{-\infty}^{\infty} f(t) f(t-k) dt = d(k) \tag{3.13.}$$

The integral in the equation is the sampled version of the following convolution integral at $t = k$ ($k \in \mathbf{Z}$).

$$\int_{-\infty}^{\infty} f(t) f(t-t) dt = f(t) * f(-t) \tag{3.14.}$$

Fourier transforming both sides of the Equation (3.13.) we get

$$\sum_{\mathbf{l}=-\infty}^{\infty}\left|\Phi\left(w-2p\,\mathbf{l}\right)\right|^2=1 \qquad (3.15.)$$

Consequently, using this condition it is possible to generate an orthogonal scaling function from an arbitrary function. Consider that we want to produce orthogonal scaling function from the function; $r(t)$. Suppose $f(t)$ and $r(t)$ are related and this relation in the frequency domain is as follows.

$$\Phi(w)=K(w)\,R(w) \qquad (3.16.)$$

Equation (3.16.) is satisfied when

$$K(w)=\frac{1}{\left(\sum_{\mathbf{l}=-\infty}^{\infty}\left|R\left(w-2p\,\mathbf{l}\right)\right|^2\right)^{1/2}} \qquad (3.17.)$$

Naturally, this is true if $\sum_{\mathbf{l}=-\infty}^{\infty}\left|R\left(w-2p\,\mathbf{l}\right)\right|^2>0$.

The inter-scale coefficients of both dilation and two-scale equation contain characteristics of scaling and wavelet function. By using the orthogonality condition together with the dilation and the two-scale equation we can easily obtain properties of the inter-scale coefficients as it is shown in the following.

$$\begin{aligned}
&\int_{-\infty}^{\infty} f(t)f(t-k)\,dt && = \\
&2\int_{-\infty}^{\infty}\sum_{m=-\infty}^{\infty}p(m)f\left(2t-m\right)\sum_{\mathbf{l}=-\infty}^{\infty}p(\mathbf{l})f\left(2t-2k-\mathbf{l}\right)dt && = \\
&\sum_{m=-\infty}^{\infty}\sum_{\mathbf{l}=-\infty}^{\infty}p(m)\,p(\mathbf{l})\cdot 2\int_{-\infty}^{\infty}f\left(2t-m\right)f\left(2t-2k-\mathbf{l}\right)dt && = \sum_{\mathbf{l}=-\infty}^{\infty}p\left(\mathbf{l}+2k\right)p(\mathbf{l}) \\
& && = d(k)
\end{aligned}$$

It is not difficult to see that a similar result is obtained when orthogonality of the translated wavelets are considered.

$$\sum_{\mathbf{l}=-\infty}^{\infty} q(\mathbf{l}+2k)\,q(\mathbf{l}) = d(k)$$

and similarly,

$$\begin{aligned}
&\int_{-\infty}^{\infty} y(t) f(t-k)\,dt && = \\
&2\int_{-\infty}^{\infty} \sum_{m=-\infty}^{\infty} q(m) f(2t-m) \sum_{\mathbf{l}=-\infty}^{\infty} p(\mathbf{l}) f(2t-2k-\mathbf{l})\,dt && = \\
&\sum_{m=-\infty}^{\infty} \sum_{\mathbf{l}=-\infty}^{\infty} q(m)\,p(\mathbf{l}) \cdot 2\int_{-\infty}^{\infty} f(2t-m) f(2t-2k-\mathbf{l})\,dt && = \sum_{\mathbf{l}=-\infty}^{\infty} q(\mathbf{l}+2k)\,p(\mathbf{l}) \\
& && = 0
\end{aligned}$$

The high pass and low pass filters are not independent of each other (Strang et al, 1996), in time domain if

$$q(k) = (-1)^k p(1-k) \tag{3.18.}$$

is chosen, the above conditions are satisfied (Strang et al, 1996). The relation between the inter-scale coefficients of scaling and wavelet function allows to construct wavelet from the inter-scale coefficients of the scaling function.

In the frequency domain Equation (3.18.) could be expressed as;

$$G(w) = e^{-jw} H^*(w+p) \tag{3.19.}$$

The low pass and high pass filters could be obtained using Equation (3.20.) and Equation (3.21.);

$$p(k) = \left\langle f(t), \sqrt{2} f(2t-k) \right\rangle \tag{3.20.}$$

and

$$q(k) = \left\langle y(t), \sqrt{2} f(2t-k) \right\rangle \tag{3.21.}$$

3.4. Properties of Bi-orthogonal Multiresolution System and Generating a Biorthogonal System

Wavelets are generally orthogonal basis functions, though there have been bi-orthogonal wavelet functions too. Orthogonality results in complicated design equations and prevents linear phase analysis. We can eliminate these problems by using bi-orthogonal wavelet bases. In bi-orthogonal MRA there are two different functions in which the responsibilities of analysis and synthesis are delegated and also two different scaling function $f(t)$ and $\tilde{f}(t)$ generate scaling subspaces V_j and $\tilde{V}_j$ respectively. And similarly there are two different wavelet function $y(t)$ and $\tilde{y}(t)$ which generate two different wavelet spaces of W_j and $\tilde{W}_j$ respectively. $\tilde{f}(t)$ is the dual scaling function and $\tilde{y}(t)$ is the dual wavelet function. The dual basis are bi-orthogonal and the two MRAs are said to be bi-orthogonal to each other such that; $V_j \perp \tilde{W}_j$ and $\tilde{V}_j \perp W_j$. In other words,

$$\left\langle \tilde{f}, y(\cdot - k) \right\rangle = 0 \quad \textit{and} \quad \left\langle f, \tilde{y}(\cdot - k) \right\rangle = 0$$

Moreover, the dual functions also have to satisfy the following expression;

$$\left\langle \tilde{f}, f(\cdot - k) \right\rangle = d_{k,0} \quad \textit{and} \quad \left\langle \tilde{y}, y(\cdot - k) \right\rangle = d_{k,0}$$

The bi-orthogonal wavelets must satisfy the following requirements; the inner product of wavelet function and its bi-orthogonal pair is equal to;

$$\left\langle y(t), \tilde{y}(t-k) \right\rangle = d(k)$$

And also the inner product of wavelet function and bi-orthogonal pair of the scaling function and the inner product of bi-orthogonal pair of wavelet function and scaling function are equal to zero.

$$\left\langle y(t), \tilde{f}(t-k) \right\rangle = 0$$

$$\left\langle \tilde{y}(t), f(t-k) \right\rangle = 0$$

While dealing with bi-orthogonal systems, the dual basis is given in terms of the dual scaling and wavelet function. They generate another multiresolution analysis of $L^2(\square)$(Gesztesy et al, 1999). The properties of the bi-orthogonal spaces can be written as;

i.) $\cdots \subset \tilde{V}_{-2} \subset \tilde{V}_{-1} \subset \tilde{V}_0 \subset \tilde{V}_1 \subset \tilde{V}_2 \subset \cdots$

ii.) $\overline{\bigcup_{j \in Z} \tilde{V}_j} = L^2(\square) \quad \bigcap_{j \in Z} \tilde{V}_j = \{0\}$

iii.) $\tilde{V}_j = \tilde{V}_{j-1} \oplus \tilde{W}_{j-1}$

iv.) $\forall j \geq j_0, \qquad L^2(0,1) = V_j \oplus \tilde{V}_j^{\perp}$

If we want to extract approximation and detail coefficients, bi-orthogonal complement of the scaling and wavelet functions should be employed. The two-scale equation for dual scaling and wavelet function is arranged as follows;

$$\tilde{f}(t) = \sum_{-\infty}^{\infty} a_k \tilde{f}(2t-k)$$

$$\tilde{y}(t) = \sum_{-\infty}^{\infty} b_k \tilde{y}(2t-k)$$

As it has been done in orthogonal case the bi-orthogonality condition for the dual scaling functions can be written as in the following.

$$\sum_{\mathbf{l}=-\infty}^{\infty} \Phi(w-2p\mathbf{l})\tilde{\Phi}^{*}(w-2p\mathbf{l}) = 1$$

Accordingly, the dual orthogonal scaling function can be obtained with this relation. Suppose that we want to produce dual scaling function from the function; $f(t)$. Suppose $f(t)$ and $\tilde{f}(t)$ are related and this relation in the frequency domain is as follows.

$$\tilde{\Phi}(w) = K(w)R(w) \qquad (3.22.)$$

The bi-orthogonality in frequency domain (Equation 3.19.) is satisfied when

$$K(w) = \frac{1}{\sum_{\mathbf{l}=-\infty}^{\infty} \left|\Phi(w-2p\mathbf{l})\right|^2}$$

Of course, this is valid when $\sum_{\mathbf{l}=-\infty}^{\infty} \left|\Phi(w-2p\mathbf{l})\right|^2 > 0$ .Thus,

$$\overline{\Phi}(w) = \frac{\Phi(w)}{\sum_{l=-\infty}^{\infty} |\Phi(w - 2pl)|^2}$$

The relationship between the inter-scale coefficients of bi-orthogonal MRA contains characteristics of dual scaling and wavelet functions. By using the b-orthogonality conditions together with the dilation and the two-scale equations we can easily obtain properties of the inter-scale coefficients as it is shown in the following.

$$\begin{aligned}
&\int_{-\infty}^{\infty} f(t)\overline{f}(t-k)\,dt && = \\
&2\int_{-\infty}^{\infty} \sum_{m=-\infty}^{\infty} p(m) f(2t-m) \sum_{\mathbf{l}=-\infty}^{\infty} \overline{p}(\mathbf{l})\overline{f}(2t-2k-\mathbf{l})dt && = \\
&\sum_{m=-\infty}^{\infty}\sum_{\mathbf{l}=-\infty}^{\infty} p(m)\overline{p}(\mathbf{l})\cdot 2\int_{-\infty}^{\infty} f(2t-m)\overline{f}(2t-2k-\mathbf{l})\,dt && = \sum_{\mathbf{l}=-\infty}^{\infty} p(\mathbf{l}+2k)\overline{p}(\mathbf{l}) \\
& && = d(k)
\end{aligned}$$

It is not difficult to see that a similar result is obtained for the inter-scale coefficients of the dual wavelet basis.

$$\sum_{\mathbf{l}=-\infty}^{\infty} \overline{q}(\mathbf{l}+2k)\,q(\mathbf{l}) = d(k)$$

With similar approach,

$$\int_{-\infty}^{\infty} y(t)\,\overline{f}(t-k)\,dt =$$

$$2\int_{-\infty}^{\infty}\sum_{m=-\infty}^{\infty} q(m) f(2t-m)\sum_{\mathbf{l}=-\infty}^{\infty}\overline{p}(\mathbf{l})\,\overline{f}(2t-2k-\mathbf{l})dt =$$

$$\sum_{m=-\infty}^{\infty}\sum_{\mathbf{l}=-\infty}^{\infty} q(m)\,\overline{p}(\mathbf{l})\cdot 2\int_{-\infty}^{\infty} f(2t-m)\,\overline{f}(2t-2k-\mathbf{l})\,dt = \sum_{\mathbf{l}=-\infty}^{\infty} q(\mathbf{l}+2k)\,\overline{p}(\mathbf{l})$$

$$= 0$$

and obviously the following can be immediately written

$$\sum_{\mathbf{l}=-\infty}^{\infty}\overline{q}(\mathbf{l}+2k)\,p(\mathbf{l})=0$$

The high pass and low pass filters are not independent of each other, in time domain if

$$q(k)=(-1)^k\,\overline{p}(k-1)$$

$$\overline{q}(k)=(-1)^k\,p(k+1)$$

In the frequency domain these are

$$Q(w)=-e^{-jw}\overline{P}(w-p)$$

$$\overline{Q}(w)=-e^{jw}P(w-p)$$

We recall the Fourier transform of the dilation equation:

$$\Phi(w)=\frac{1}{\sqrt{2}}P\left(\frac{w}{2}\right)\Phi\left(\frac{w}{2}\right) \qquad (3.23.)$$

We substitute $\hat{\Phi}(w) = K(w)\Phi(w)$ in Equation (3.23.) and we obtain

$$\hat{\Phi}(w) = \frac{1}{\sqrt{2}} K(w) K^{-1}\left(\frac{w}{2}\right) P\left(\frac{w}{2}\right) \hat{\Phi}\left(\frac{w}{2}\right)$$

Then we get

$$\hat{\Phi}(w) = \frac{1}{\sqrt{2}} \hat{P}\left(\frac{w}{2}\right) \hat{\Phi}(\frac{w}{2})$$

with

$$\hat{P}(w) = \frac{K(2w)}{K(w)} P(w)$$

The corresponding two-scale equations of the wavelets are then

$$\Psi(w) = \frac{1}{\sqrt{2}} Q\left(\frac{w}{2}\right) \Phi\left(\frac{w}{2}\right) \tag{3.24.}$$

$$\hat{\Psi}(w) = \frac{1}{\sqrt{2}} \hat{Q}\left(\frac{w}{2}\right) \hat{\Phi}\left(\frac{w}{2}\right) \tag{3.25.}$$

where $Q(w)$ and $\hat{Q}(w)$ are defined in Equation (3.24.) and Equation (3.25.) respectively. In time domain,

$$y(t) = \sqrt{2} \sum_k q(k) f(2t-k), \quad g(k) = (-1)^k \hat{p}(k-1) \tag{3.26.}$$

$$\hat{y}(t) = \sqrt{2} \sum_k \hat{q}(k) \hat{f}(2t-k), \quad \hat{q}(k) = (-1)^k p(k+1)$$

The dilation equations of the scaling functions are also reproduced in the following.

$$f(t) = \sqrt{2}\sum_{k} p(k) f(2t-k), \tag{3.27.}$$

$$\tilde{f}(t) = \sqrt{2}\sum_{k} \tilde{p}(k) \tilde{f}(2t-k) \tag{3.28.}$$

When we compare orthogonal and bi-orthogonal wavelets, we can figure out some differences. First, in orthogonal wavelets the length of scaling and wavelet filter have to be equal and even, but in bi-orthogonal wavelets there is not any restriction about this condition. Second, we can say that in bi-orthogonal wavelets, wavelets and scaling functions can be symmetric. As a third manner, while orthogonal wavelets preserve the energy in the time domain and frequency domain, bi-orthogonal wavelets don't satisfy this condition. Also we can define that bi-orthogonal wavelets don't produce a perfect absolute magnitude response. They amplify or attenuate the most frequency components. We can switch the role of primary and dual filters in bi-orthogonal wavelets. We can compute the expansion coefficients simply in orthogonal systems.

3.5. Wavelet Families

There have been large number of known wavelet families and functions and they provide a rich space in which to search for a wavelet which will very efficiently represent a signal of interest in a large variety of applications. We can define many basis functions to use as the mother wavelet for Wavelet Transformation. Since the mother wavelet produces all wavelet functions used in the transformation through translation and scaling, it determines the characteristics of the resulting WT. Therefore, the details of the particular application should be considered and the appropriate mother wavelet should be chosen in order to use the WT effectively.

In this thesis, we employed some well-known wavelet families and in the following paragraph we briefly gave information about them. The other wavelet families that not used in this thesis could not be explained.

The most popular wavelet family is the Daubechies wavelets. They represent the foundations of wavelet signal processing and are used in numerous applications. These are also called Maxflat wavelets as their frequency responses have maximum flatness at frequencies 0 and π. This is a very desirable property in some applications. The names of the Daubechies family wavelets are written dbN, where N is the order, and db is the "surname" of the wavelet. The length of the scaling and wavelet filter is 2N. The support length of wavelet and scaling function is $2N - 1$. In Figure 3.4, wavelet and scaling function of the dB4 wavelet are shown.

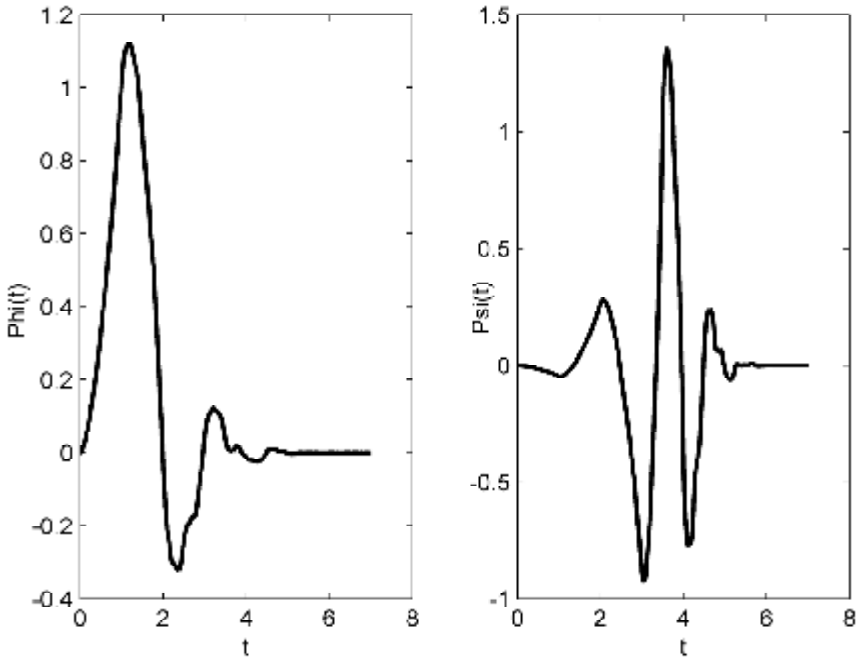

Figure 3.4. Illustration of scaling (left) and wavelet (right) functions of dB4 wavelet

We can represent a signal by using any member of Daubechies family. They are similar in shape to QRS complex and their frequency spectrum is concentrated around low frequencies like ECG signal. As it is orthogonal there is a scaling function which generates multi resolution analysis (Nick et al, 1997). Any

Daubechies wavelet is defined by its vanishing moments or no of zero moments.

First we found a progression $\{a_k; k \in Z\}$ that satisfy the following four conditions for all integer $N \geq 2$;

$$a_k = 0 \quad if \quad k < 0 \quad or \quad k > 2N$$

$$\sum_{k=-\infty}^{\infty} a_k a_{k+2m} = d_{0m} \; for \quad all \quad m$$

$$\sum_{k=-\infty}^{\infty} a_k = \sqrt{2}$$

$$\sum_{k=-\infty}^{\infty} b^k k^m = 0, \quad 0 \leq m \leq N-1$$

where

$$b_k = (-1)^k a_{-k+1}$$

$If \quad N = 1, \quad then \quad a_0 = a_1 = 1,$ corresponding to the Haar basis.

We found a scaling function from the above progression. This function satisfies the below expression;

$\int f(t)dt = 1$ for integer N. the support of $f(t)$ is $[0, 2N-1]$.

Similarly there is wavelet function which fulfill the following;

$\int y(t)t^m dt = 0$ for all integers $0 \leq m \leq N-1$ (Daniel et al, 1994).

When we investigate the wavelet-scaling functions of Daubechies wavelets, we can figure out that they are far from symmetry. Because of this situation symlet wavelets are developed. The symlets have other properties similar to those of the dbNs.

Symlet wavelets are orthogonal and near symmetric. This property ensures minimal phase distorsion. Order N can be 2, 3 ... .They are orthogonal, biorthogonal and provide compact support. Their associated scaling filters are near linear-phase filters. Apart from the symmetry, the other properties of the Daubechies and Symlet families are similar. Symlet wavelets have p vanishing points and their scaling functions satisfy (Mallat, 1999)

$$\int_{-\infty}^{\infty} f(t)dt = 1$$

and

$$\int_{-\infty}^{\infty} t^k f(t)dt = 0 \qquad for \qquad 1 \le k \le p$$

In Figure 3.5 wavelet and scaling function for Symlet wavelet at order 4 is illustrated.

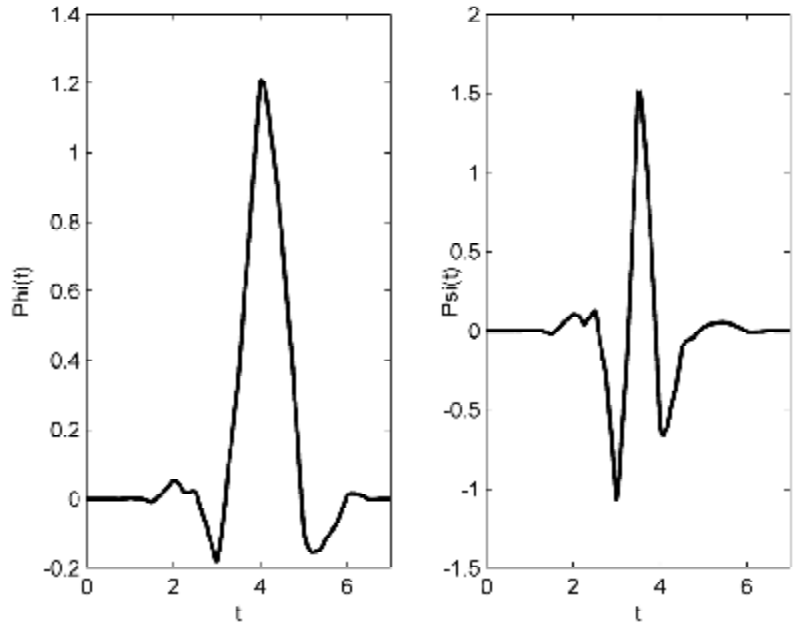

Figure 3.5.Illustration of scaling (left) and wavelet (right) functions of Sym4 wavelet

Coiflet wavelets are another most common wavelet family. Built by Daubechies at the request of Coifman, the wavelet function has 2N moments equal to 0 and, the scaling function has 2N-1 moments equal to 0. The two functions have a support of length 6N-1. They are orthogonal like Daubechies and Symlet and they are more symmetric and have more vanishing moments than the Daubechies wavelets. These are compactly supported wavelets with highest number of vanishing moments for both $_y$ and f as 2N and 2N-1 respectively. This property provides linear phase characteristics of the Coiflet wavelet (Gao, 2011).

The *coifN* wavelet and scaling function are much more symmetrical than the *dbN*s. With respect to the support length, *coifN* has to be compared to *db*3*N* or *sym3N*. With respect to the number of vanishing moments of wavelet function, *coifN* has to be compared to *db*2*N* or *sym2N*.

In Figure 3.6 wavelet and scaling function for Coiflet wavelet is illustrated.

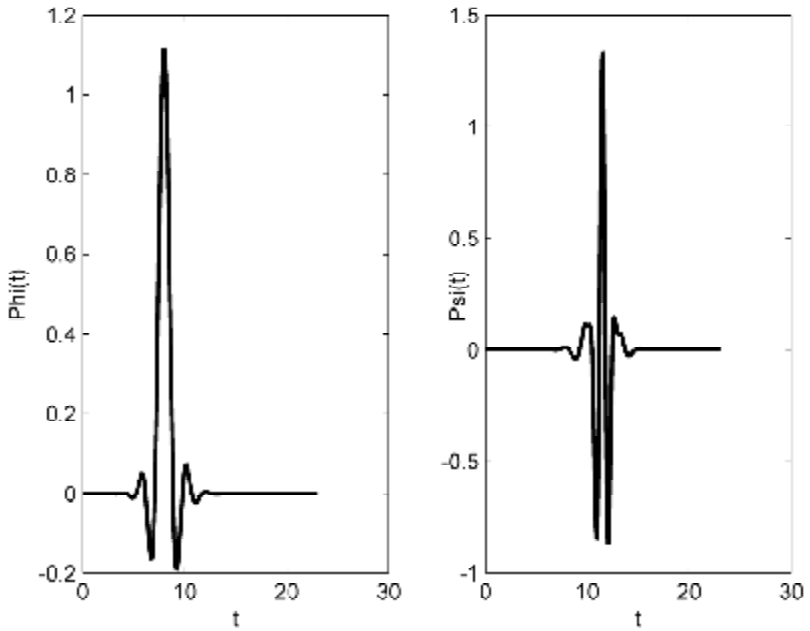

Figure 3.6.Illustration of scaling (left) and wavelet (right) functions of Coif4 wavelet

We also employed Meyer wavelet in this thesis. Meyer wavelets are capable of perfect reconstruction. We defined the Fourier transform $\Phi(w)$ of a scaling function $f(t)$ as:

$$\Phi(w) = \begin{cases} 1 & \text{if} \quad |w| \le \frac{2}{3}p \\ \cos\left[\frac{p}{2}v(\frac{3}{4p}|w|-1\right] & \text{if} \quad \frac{2}{3}p \le |w| \le \frac{4}{3} \\ 0 & \text{otherwise} \end{cases}$$

where *v* is a smooth function which satisfy the following;

$$v(t) = \begin{cases} 0 & \text{if } t \le 0 \\ 1 & \text{if } t \ge 1 \end{cases}$$

with

$$v(t) + v(1-t) = 1$$

and wavelet function could be found from the scaling function. In Figure 3.7 wavelet and scaling function for Meyer wavelet is illustrated.

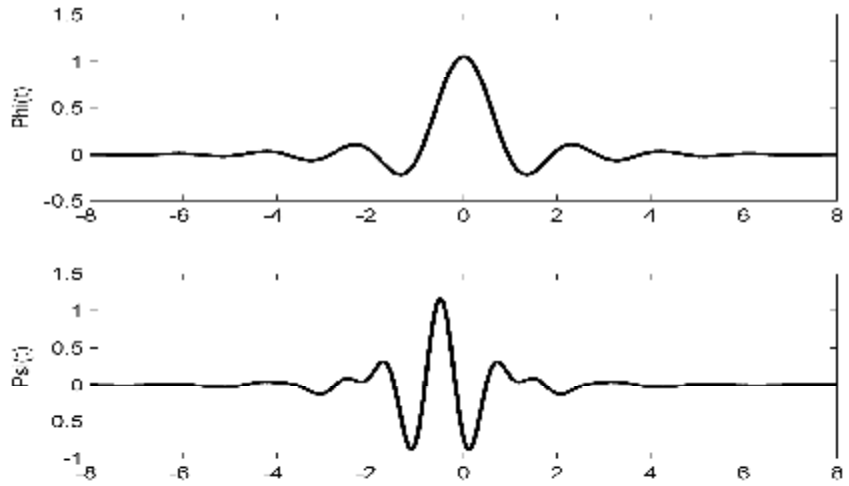

Figure 3.7.Illustration of scaling and wavelet functions of Meyer wavelet

3.6. Two Band Filter Banks and Their Relation with Multiresolution Analysis

A filter bank is set of filters. A two-channel filter bank is shown in the figure 3.5. In a two-channel filter bank, a signal is composed into two parts by two linear filters; one is low-pass and the other is high-pass are followed by 2-fold down sampler. This is the analysis section of the filter bank system. Each of the two outputs of the analysis part is up-sampled by 2-fold up-sampler preceded by a filter and the outputs of these filters are summed to re-constitute the signal. This part is the analysis section.

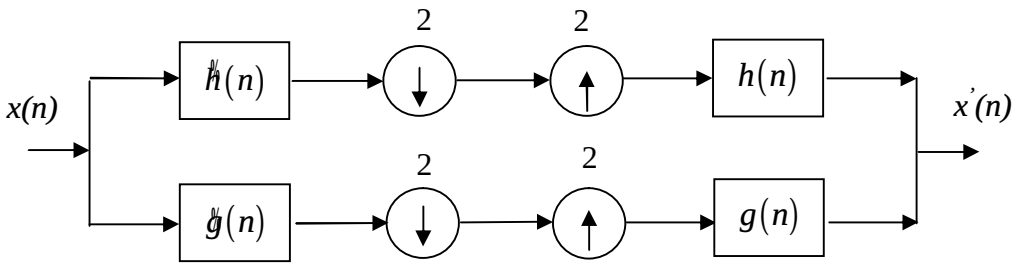

Figure 3.8.Structure of Two-channel Filter

Investigating the two-band filter bank in z -domain we see that the following equations should be satisfied for perfect reconstruction in the syntheses part.

$$G(z) = -zH(-z) \tag{3.29.}$$

$$G(z) = -z^{-1}H(-z) \tag{3.30.}$$

These chooses lead to

$$H(z)H(z) + H(-z)H(-z) = 2 \tag{3.31.}$$

$$\tilde{G}(z)G(z)+\tilde{G}(-z)G(-z)=2 \tag{3.32.}$$

Note that if the term z^{-1} was not absent in Equations (3.31.), we would reach to;

$$\tilde{H}(z)H(z)-\tilde{H}(-z)H(-z)=2\,.$$

which is not the desired result. The Equations (3.31.) and (3.32.) in time domain becomes;

$$\sum_{n=-\infty}^{\infty}\tilde{h}(n)h(2k-n)=d(k) \tag{3.33.}$$

$$\sum_{n=-\infty}^{\infty}\tilde{g}(n)g(2k-n)=d(k) \tag{3.34.}$$

Consequently, if Equation (3.33.) and Equation (3.34.) are satisfied the filter bank reconstructs perfectly the analyzed signal at the syntheses part.

The results obtained here can be easily adapted to multi-resolution analysis. Here, the role of $\tilde{h}(n)$ and $h(n)$ are replaced by $\tilde{p}(n)$ and $p(n)$ respectively and the role of $\tilde{g}(n)$ and $g(n)$ are replaced by $\tilde{q}(n)$ and $q(n)$ respectively. The frequency domain correspondence of the Equation (3.29.) and Equation (3.30.) can be written by replacing the variable z by e^{jw} ;

$$\tilde{G}(w)=-e^{jw}H(w-p) \tag{3.35.}$$

$$G(w)=-e^{-jw}\tilde{H}(w+p) \tag{3.36.}$$

which is in parallel with Equations (3.35.) and (3.36.) as expected.

These choices are equivalent to the selection $G(z) = -zH(-z^{-1})$. In frequency domain this is $G(w) = -e^{jw} H(p - w)$ which is the quadrature mirror of $H(w)$. And in the time domain we have $g(n) = -(-1)^n h(-1-n)$. This requirement provides that all the filters in the orthogonal filter bank depend on the low-pass analysis filter $h(n)$.

The DWT is computed by successive low-pass and high-pass filtering as shown in Figure 3.9. This is called the Mallat algorithm or Mallat-tree decomposition. It connects the continuous-time multiresolution to discrete-time filters. In the figure, the signal is denoted by the sequence *x(n)* (Addison, 2002). The low-pass and high-pass filtering branches of the filter bank retrieve respectively the approximations and details of the signal *x(n)*. We can expand the filter bank to an arbitrary level, depending on the desired resolution.

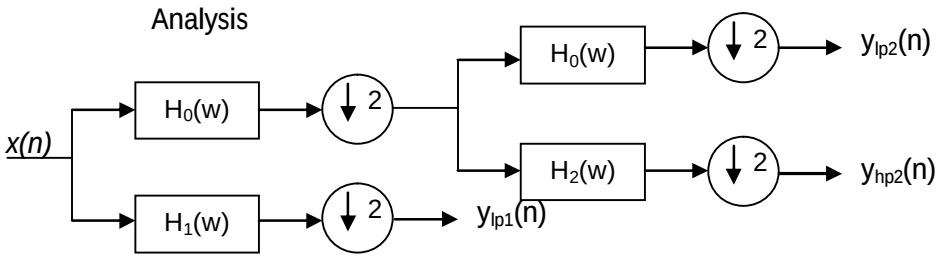

Figure 3.9.Two-level wavelet decomposition tree (Semmlov, 2004)

The inverse discrete wavelet transform (IDWT) reconstructs a signal from the approximation and detail coefficients derived. At each decomposition level, the half band filters produce signals which span only half the frequency band. With this method, the time resolution becomes good at high frequencies, while the frequency resolution becomes good at low frequencies. The filtering and decimation process is continued until the desired level is reached. The maximum number of levels depends on the length of the signal. The DWT of the original signal is then obtained by starting from the last level of decomposition.

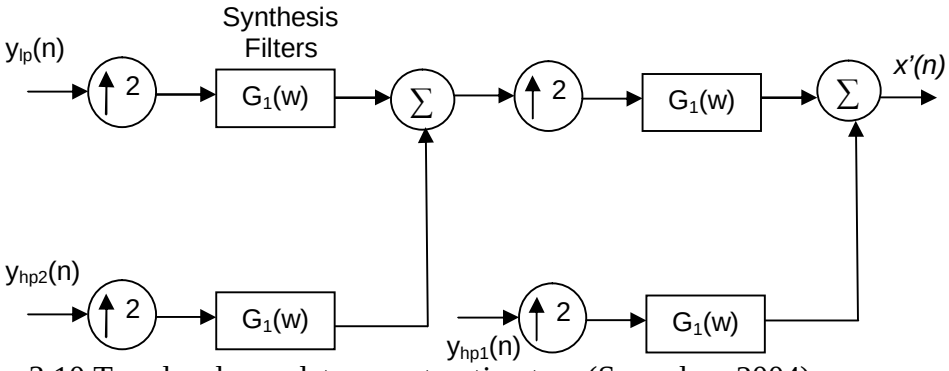

Figure 3.10.Two-level wavelet reconstruction tree (Semmlov, 2004)

In Figure 3.10, we can see the reconstruction process of the original signal from wavelet coefficients. The reconstruction process is the reverse of decomposition process. At each level approximation and detail coefficients are upsampled by two, passed through low pass and high pass filters and then added. Till obtaining the original signal this process is continued (Addison, 2002).

4. FINDINGS AND DISCUSSIONS

4.1. Custom Multiresolution System

This chapter presents the results and discussions which are obtained during the project.

The algorithm was realized by using Matlab (Mathworks Inc.), and Matlab's wavelet, signal processing, optimization and statistical toolboxes.

A QRS signal looks like as in Figure 4.1. This QRS signal has been obtained by ensemble averaging the detected QRS complexes in the database used in this study.

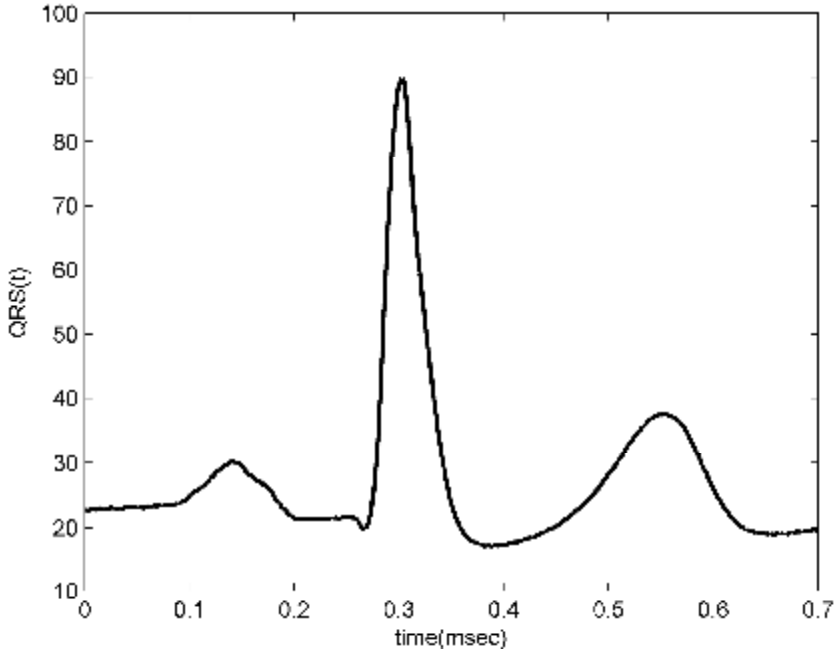

Figure 4.1.QRS signal of an ECG signal

The power spectrum of the QRS signal shown in Figure 4.1 is shown in Figure 4.2. We can easily notice from this figure that the most concentrated part of the spectrum lies between 1Hz and 40Hz.

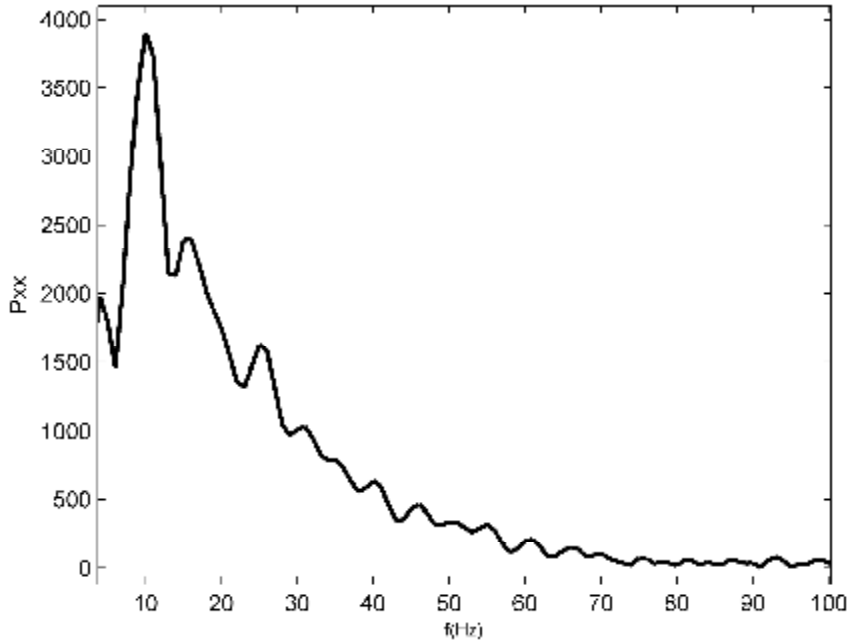

Figure 4.2.Half cycle (0 Hz-500 Hz) of the Power Spectrum of the QRS signal

Since the sampling frequency is 1000 Hz and the cut-off frequency of the low pass filter that employed is 50 Hz, the depth of the wavelet is computed as;

$$\log_2(500/50) = 3.32$$

So we took J=3. We determined a function which resembles to an R peak to construct a scaling function. We express this function as below and Figure 4.3 shows it's graphic on time domain.

$$r(t) = a^{2t} e^{(-at)} u(t) \qquad (4.1.)$$

where $a = 2$ and the function $u(t)$ is chosen to have unit area.

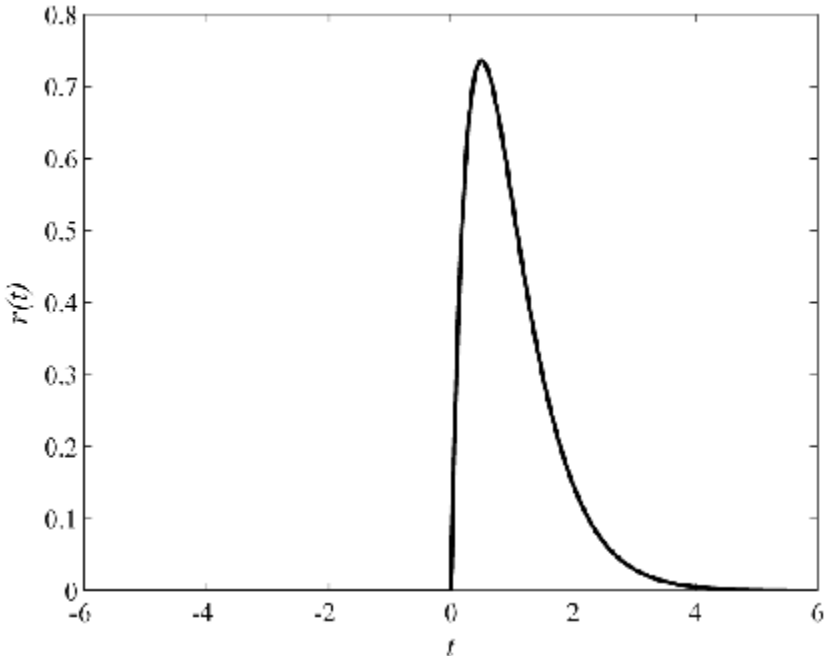

Figure 4.3.Plot of the r(t) Function for a=2

The Fourier transform of our function $R(w)$ could be expressed as in Equation (4.2.).

$$R(w) = a^2 \frac{1}{(jw+a)^2} \tag{4.2.}$$

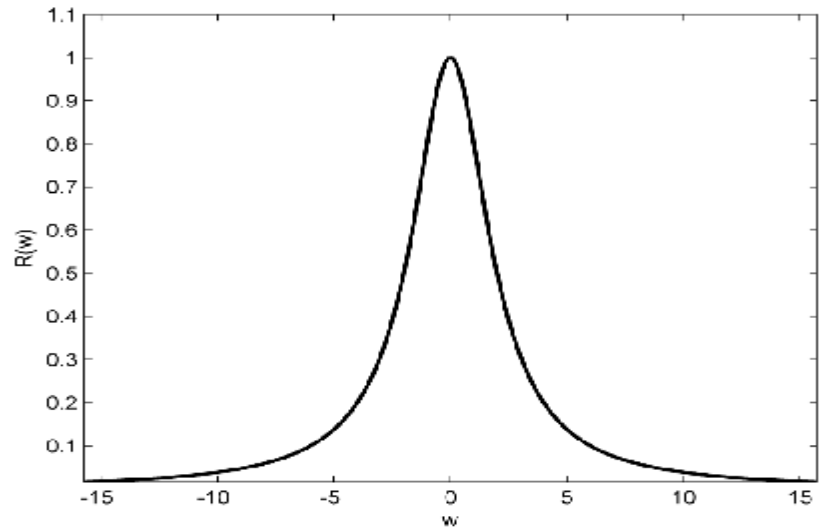

Figure 4.4.Fourier Transform of the r(t) for a=2

We can determine the magnitude function of the $R(w)$ as in Equation (4.3.) and the plot of it as in Figure 4.5.

$$M(w) = |R(w)| = a^2 \frac{1}{(w^2 + a^2)} \tag{4.3.}$$

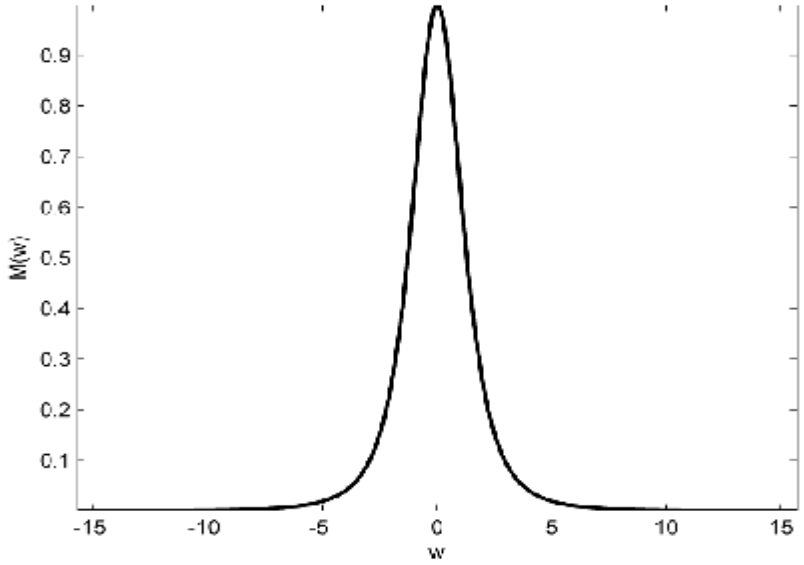

Figure 4.5.Magnitude function of the *R(w)* for a=2

We orthogonalized this function with following the steps given in Section 3. In Figure 4.6 graphical representation of *K(w)* and *b(w)* of Equation (3.14.) are given. *b(w)* is the denominator of Equation (3.17.).

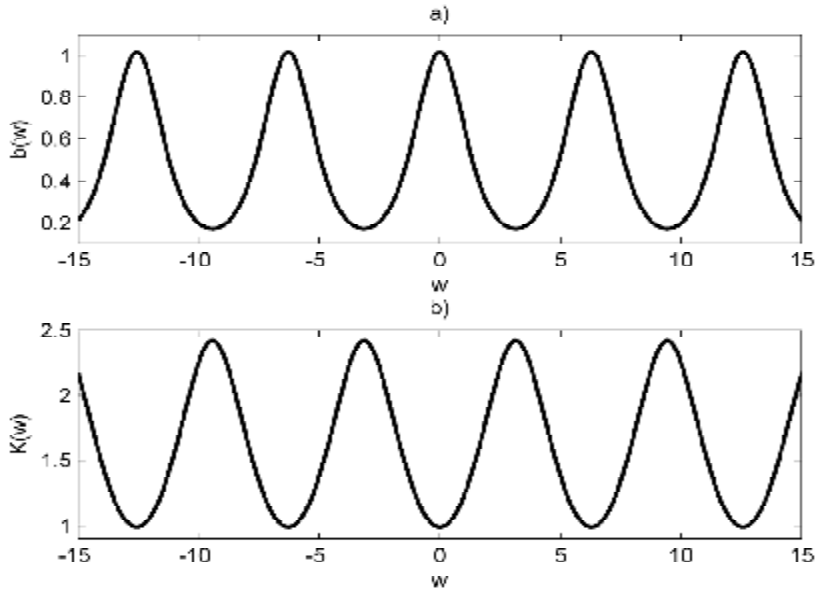

Figure 4.6.Grapfh of b(omega) and K(omega)

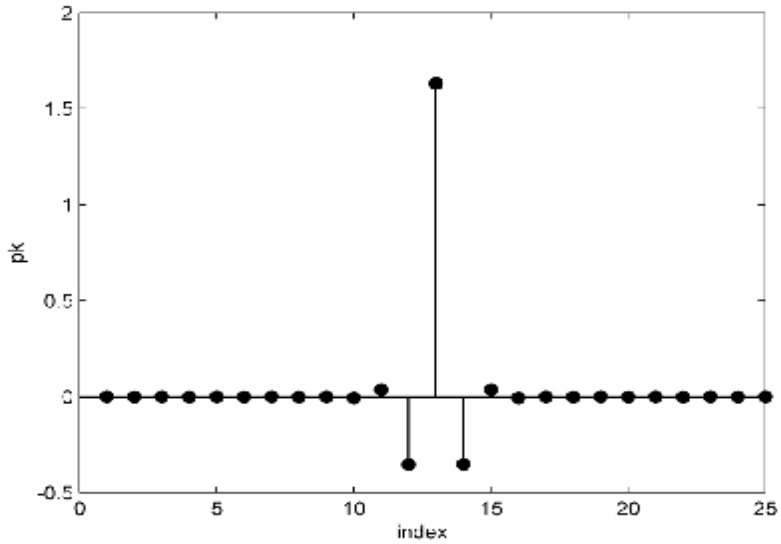

Figure 4.7.Fourier Series Coefficients of the orthogonalized scaling function

From Equation (3.17.) we computed many interscale coefficients p_k which is necessary to compute discrete wavelet transform. The graphical representation of this sequence is given in Figure 4.7. The corresponding orthogonal scaling function is extracted by Equation (3.24.) and it is shown in Figure 4.8.

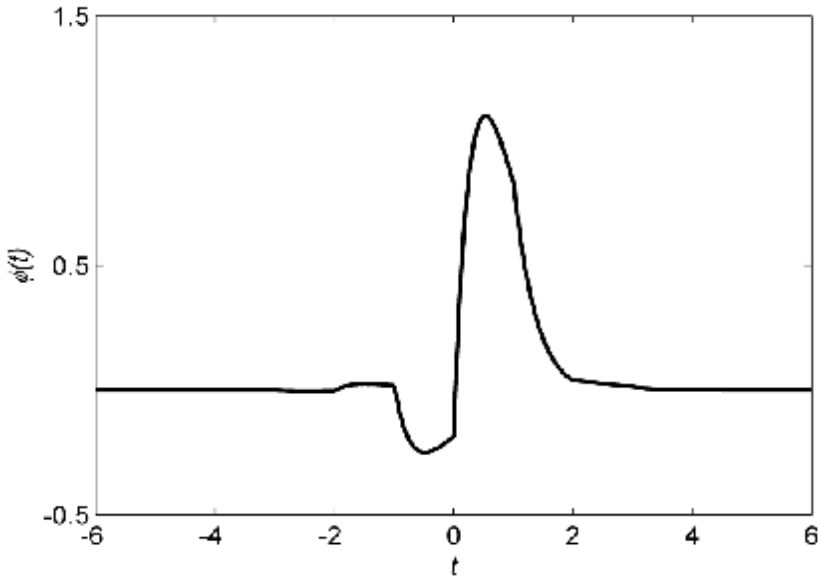

Figure 4.8.Orthogonalized Scaling Function

As described in Chapter 3, the interscale coefficients of the orthogonal system provide low pass filter coefficients p_k and high pass filter coefficients q_k. However these sequences are infinite length and need to be cropped with a rectangular window for practical use. As $|k|$ increases the values of the sequence p_k decreases (Figure 4.8). It looks reasonable to keep the coefficients with indexes $k = -15\mathbf{K}16$ and abandon the others because they are relatively small. The computational errors and the cropping violate the orthogonality. So we apply fine tuning to the filter coefficients p_k; we employ non-linear constrained optimization to hold the orthogonality. The fine tuning is done with using the Optimization Toolbox of Matlab. The optimization does not change the coefficients of much since the removed coefficients do not contribute much energy in the sequence. Mean square error of the coefficients before and after fine tuning is computed as 2.22e-005. The low pass filter coefficients obtained from the tuned p_k via Equation 3.20 and high pass filter coefficients obtained from q_k via Equation 3.21 are shown in Figure 4.9.

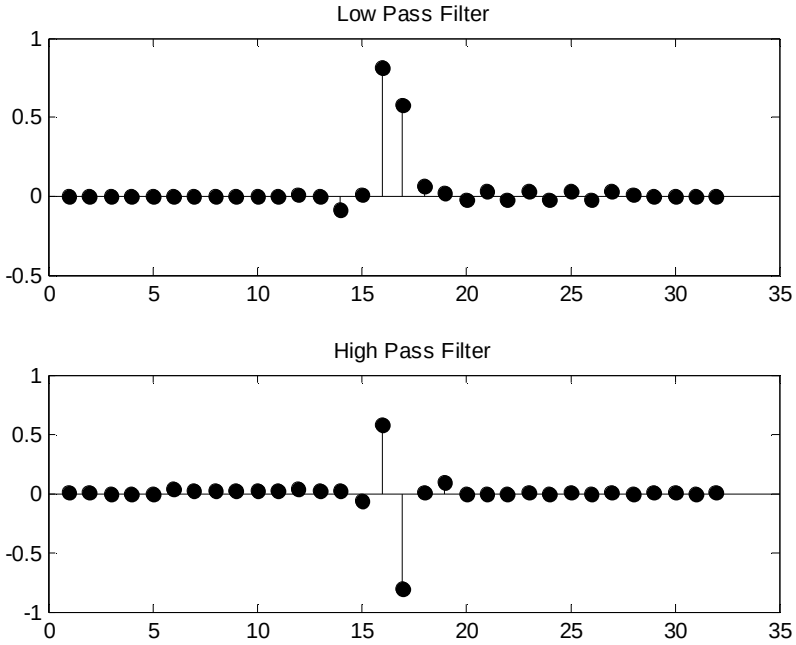

Figure 4.9.Low Pass and High Pass Filters of custom multirate system

The frequency response of the low pass and high pass filters are also shown in Figure 4.10 and Figure 4.11 respectively.

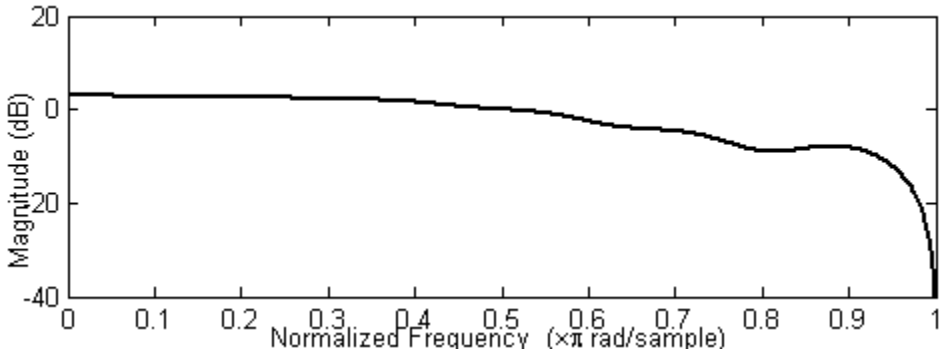

Figure 4.10.Frequency Response of the Low Pass Filter

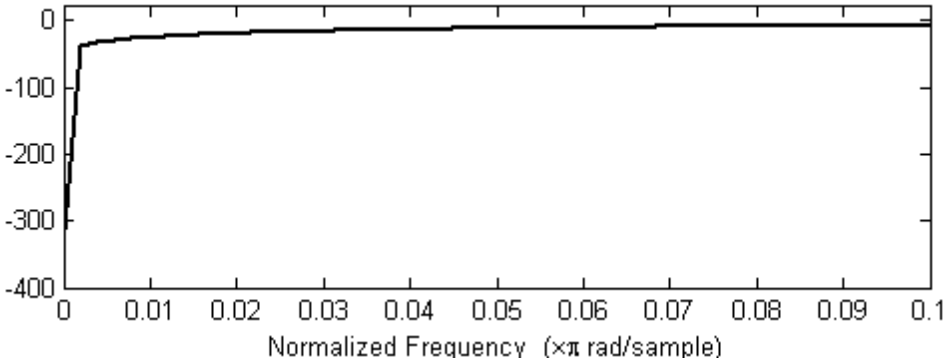

Figure 4.11.Frequency Response of the High Pass Filter

Since we have the high pass filter coefficients, we can compute the corresponding wavelet of the orthogonal scaling function from Equation (3.23.). The plots of q_k and the orthogonal wavelet are in Figure 4.12 and Figure 4.13 respectively.

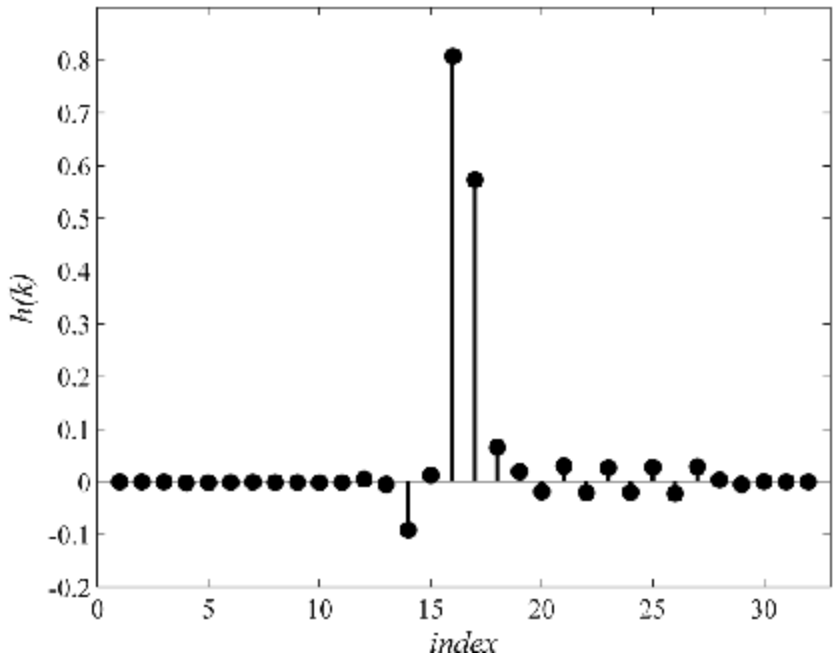

Figure 4.12.Coefficients for Constructing Wavelet from Desired Scaling Function

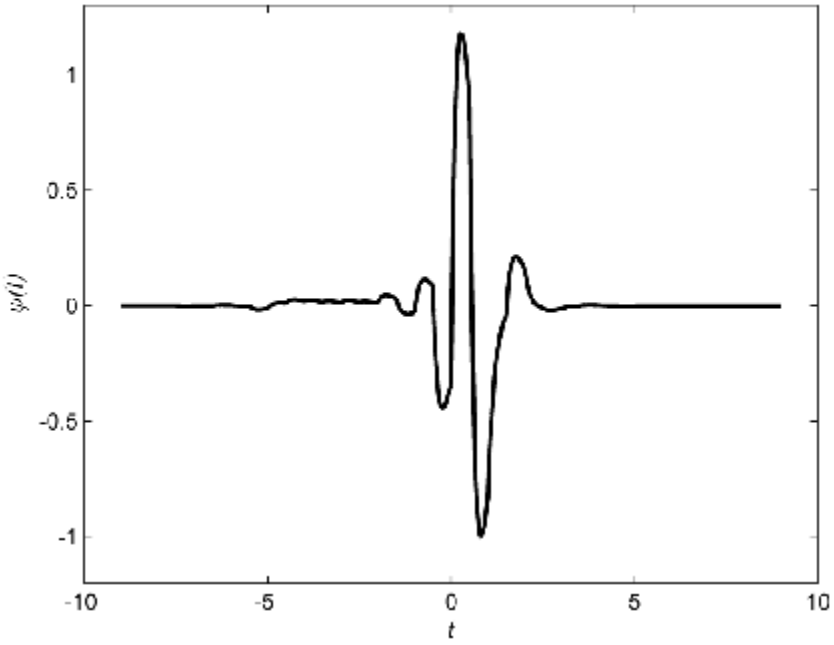

Figure 4.13. Wavelet Function corresponding to the orthogonalized scaling function

4.2. QRS Detection Algorithm

The scheme of QRS detection (actually R peak detection) algorithm is sketched in Figure 4.14.

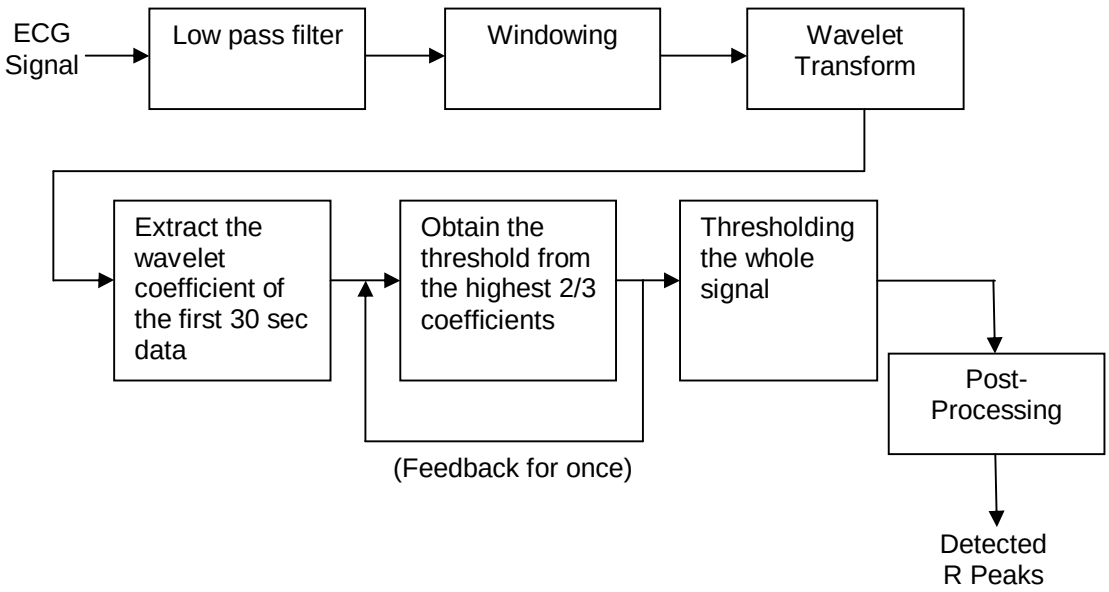

Figure 4.14.The QRS Detection Procedure

The first stage of the QRS detection procedure is digital FIR filter. In this stage a FIR low pass filter with order 20 (length is 21) and cutoff frequency of 50 Hz is employed. The graphical representation of the FIR filter's frequency response is shown in Figure 4.15.

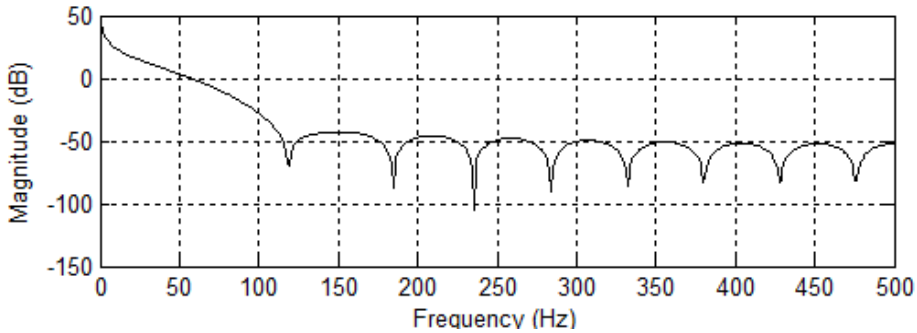

Figure 4.15.Frequency Response of the FIR Filter

The bandwidth of the filter is chosen by investigating the power spectrum of the averaged QRS complex. The power spectrum of the averaged QRS is given in the Figure 4.2. The low pass filter for the QRS detection algorithm reduces noise in the ECG signal. The filter attenuates muscular noise which resides in the high frequencies and 50 Hz power line interference and its harmonics. A raw ECG signal and filtered ECG signal before and after filtering are shown in Figure4.16 and Figure 4.17 respectively.

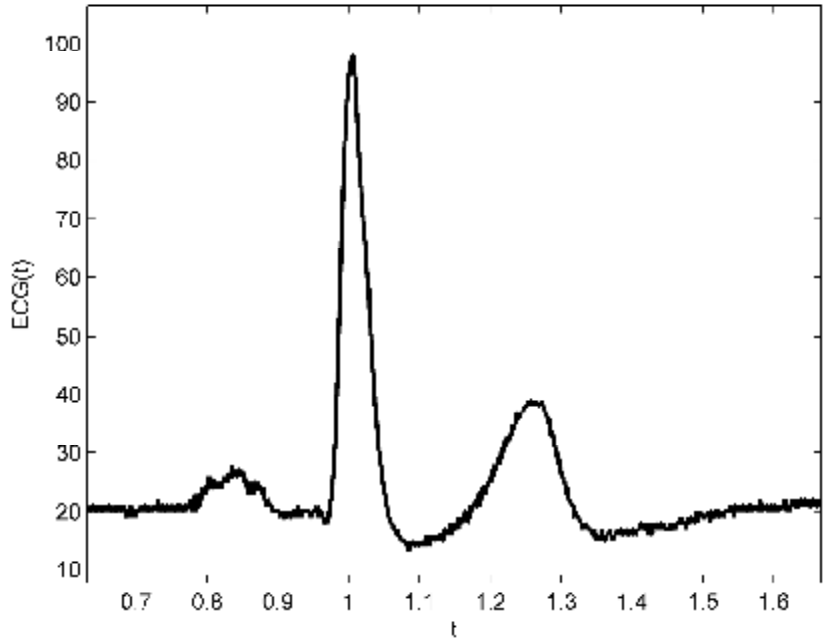

Figure 4.16.Unfiltered ECG signal

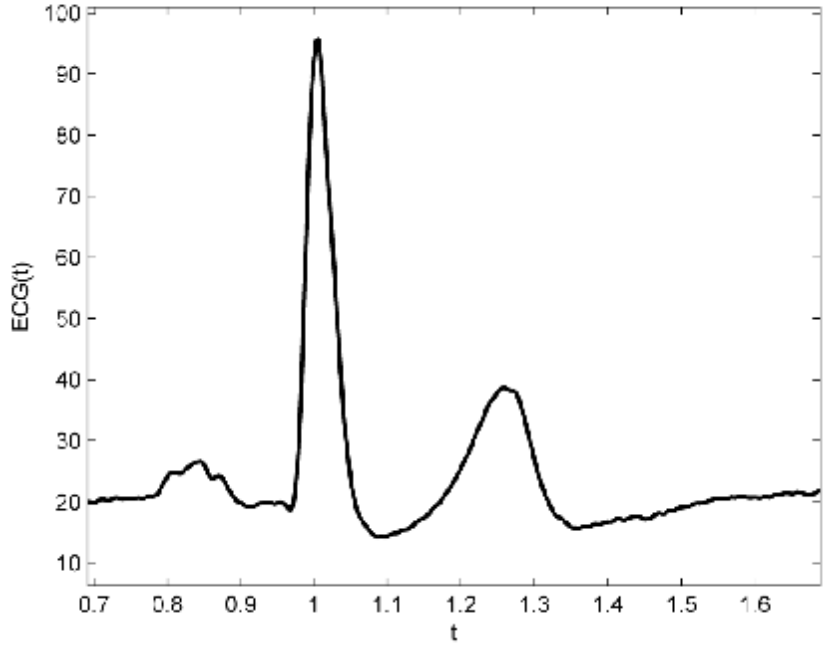

Figure 4.17.Filtered ECG signal

In the windowing stage, we specified a window which is wide enough to cover an R peak in the ECG signal. Its width is chosen as 100 samples which correspond to 0.1 second. This is also nearly equal to QRS interval. It is shifted by 10

samples to cover all R peaks. If the size of the window is too large, it will merge the QRS and T complexes together. On the other hand, if the size of the window is too small, a QRS complex could produce several peaks at the output of the stage. The data from each window is stored. Then at the end we have the ECG data set as a matrix that includes a part of ECG signal at one column. Illustration of the windowing procedure is shown in Figure 4.18.

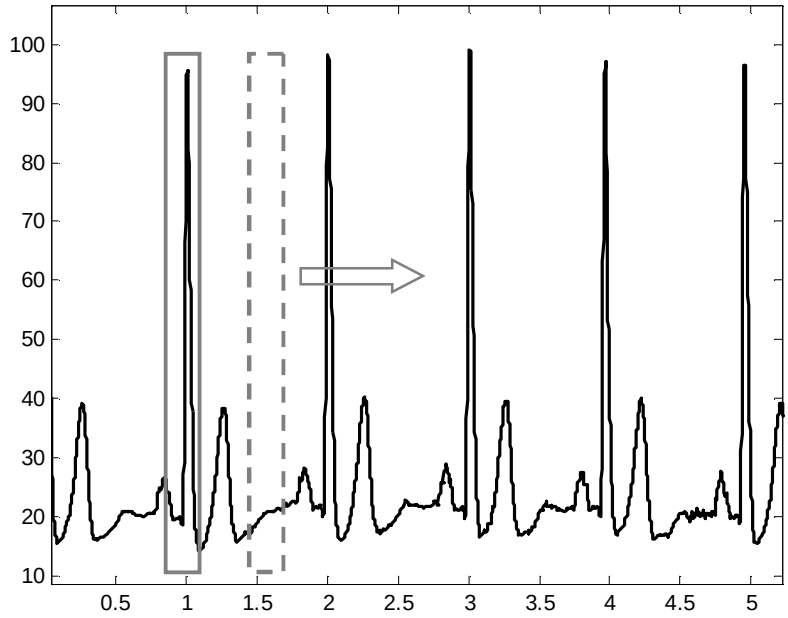

Figure 4.18.Illustration of windowing for an ECG signal.

We computed the approximation and detail coefficients of each window by using Equation (4.4.) and Equation (4.5.) respectively. For each window the wavelet coefficients;.

$$a_{j,\mathbf{l}} = \left\langle x_{\mathbf{l}}(t),\ f\left(2^{j}t - 0.01 \cdot 2^{j}\mathbf{l}\right)\right\rangle \tag{4.4.}$$

$$b_{j,\mathbf{l}} = \left\langle x_{\mathbf{l}}(t),\ y\left(2^{j}t - 0.01 \cdot 2^{j}\mathbf{l}\right)\right\rangle \tag{4.5.}$$

where ***x(t)*** is the ECG signal. And the magnitude measure from these coefficients are computed by

$$\text{mag}_{j,\mathbf{l}} = \sqrt{a_{j,\mathbf{l}}^2 + b_{j,\mathbf{l}}^2} \tag{4.6.}$$

Here, $x_{\mathbf{l}}(t) = x(t), \quad 0.01\mathbf{l} \le t < 0.01\mathbf{l} + 0.1$ is the $\mathbf{l}$ th segment of ECG signal ***x(t)***.Note that a signal segment obtained by windowing is represented by only one approximation or detail or magnitude coefficient. These coefficients are computed for each window for the first 30 second part of the ECG signal. As the shift size decreases, the resolution and the total wavelet coefficients will increase and also the computation time will increase but a segment is still represented by a single feature or value. These features are then used for detecting R peak (correspondingly QRS complex). We have three approaches for constructing features. These approaches are listed in the following:

1: Approximation coefficients are computed for each segment.

2: Detail coefficients are computed for each segment.

3: Magnitude coefficients are computed from approximation and detail coefficients as in Equation (4.6.) for each segment.

R peaks detection is the key for QRS detection because Q and S peaks occur around the R peak within 0.1second. Since R peaks are sharper than from Q and S peaks, the features related to R peaks will be higher in magnitude than the features related to Q and S peaks. Therefore, in order to extract the R peaks, thresholding is done after computing the features. A threshold level is determined and the features higher than this threshold assigned as the features corresponding to the R peaks. The threshold level is determined from the first 30 seconds data. We used soft thresholding method, so threshold level would be different for each ECG signal. First we excluded the 1/3 part of the least values of the coefficients because we assume that they are related to the noise component of the signal and they do not contribute much to the signal energy. Then, we computed the mean of remained 2/3 part for determining the threshold level. The obtained threshold level may not be sufficient to eliminate P and T peaks so it should be updated. First, the reference data is thresholded and then from the remaining features we obtain updated threshold level; we again exclude the lowest 1/3 features and compute the mean of other features.

This new threshold level is applied to whole signal and the features that do not represent R peaks are eliminated.

Post-processing stage makes sure that T waves or Q waves and S spikes have not been wrongly labeled as R peaks. Before the post processing stage we sorted the indexes which point out the place of the data on the ECG signal above the threshold level sequentially. These indexes also hold the magnitude levels of each sample. A QRS wave interval is approximately 60 ms which correspond to 60 samples because our sampling frequency is 1 KHz. At third level of the wavelet tree the samples are reduced to 60/8=7.5 samples. Therefore about 8 samples represent QRS and distance between Q and R and S and R peaks is about 8/2=4.We calculated the differences between adjacent indices of the coefficients. If the difference is less than or equal to 5, we expect that there could be a QRS complex in there and the index which points the highest value in that group is the R peak potentially. The one coefficient with high absolute value is kept and the other is eliminated, this repeated until the difference of neighborhood peaks are higher than 5. Otherwise a new QRS group would be pointed. Let two consecutive coefficients passed the threshold are $a_{j,\mathbf{l}_1}$ and $a_{j,\mathbf{l}_2}$ with $\mathbf{l}_2 > \mathbf{l}_1$. If $\mathbf{l}_2 > \mathbf{l}_1$, obtain $\mathbf{l} = \arg\max\left(\left|a_{k,\mathbf{l}_1}\right|, \left|a_{k,\mathbf{l}_2}\right|\right)$ then keep the coefficient with indice ı and remove the other. This repeated until the difference of indices of neighborhood coefficients are higher than 5. We took the value of the difference as 5 but this value is dependent to the sampling frequency of the ECG signal.

We tested proposed detector for 10 different ECG signals. Each signal has 300000 samples with sampling frequency of 1000 Hz. And also for comparison we used dB3, dB4, dB5, dB6, dB7, dB8, Sym3, Sym4, Sym5, Coif3, Coif4, Coif5 and Meyer wavelet functions.

4.3. Experimental Results

In this Section the QRS detection results are presented. We tested R peak detection performances of our scaling and wavelet function upon some different

recorded ECG signals offline by using the custom and the common wavelets like Daubechies, Symlet, Coiflet and Meyer wavelets individually and compared the results.

The results are grouped into two. The first group contains results obtained with custom wavelet and some well-known wavelets. The second result group contains the results obtained via Discrete Wavelet Transform. Two measures are employed for quantifying the performances; R1 and R2. R1 and R2 are formulated as follows;

$$R1 = \frac{\text{\# detected R peaks}}{\text{\# total R peaks}} \text{ x } 100 \tag{4.7}$$

$$R2 = \frac{\text{\# R peaks after post processing}}{\text{\# R peaks before post processing}} \text{ x } 100 \tag{4.8}$$

As the value of R2 decreases, the number of the detected false R peak number increases. R1 indicates the success of the whole algorithm while R2 provides the performance of our post processing stage.

As it can be seen from Table 4.1, the ratios of the successfully detected R peaks obtained with the custom wavelet are nearly the same for all approaches. But we can say that the success of detecting R peaks is not much without post-processing.

Table 4.1.Experimental results with custom wavelet.

			Ratio of Detected R Peaks										
ECGs / Approaches			1	2	3	4	5	6	7	8	9	10	Success
Custom Wavelet	1	R1	1	1	1	1	1	0,991	0,942	1	0,992	1	**0,993**
		R2	0,197	0,132	0,187	0,208	0,218	0,236	0,090	0,211	0,225	0,203	0,191
	2	R1	1	1	1	1	1	0,991	0,921	1	0,992	0,978	**0,988**
		R2	0,213	0,264	0,205	0,218	0,241	0,275	0,103	0,211	0,254	0,190	0,217
	3	R1	1	1	1	1	0,982	0,991	0,993	1	0,992	0,942	**0,990**
		R2	0,094	0,247	0,089	0,112	0,241	0,115	0,241	0,102	0,111	0,202	0,155

Table 4.2.Experimental results with Daubechies wavelet.

			Ratio of Detected R Peaks										
Approaches \ ECGs			1	2	3	4	5	6	7	8	9	10	Success
dB3	1	R1	0,917	1	0,939	0,829	0,789	0,981	0,847	0,979	1	0,971	**0,846**
		R2	0,223	0,264	0,219	0,241	0,075	0,164	0,149	0,213	0,262	0,200	0,201
	2	R1	1	1	1	1	1	1	0,869	1	1	0,964	**0,983**
		R2	0,225	0,272	0,218	0,254	0,256	0,294	0,146	0,226	0,274	0,206	0,237
	3	R1	0,935	1	0,980	1	0,890	1	0,861	0,958	0,968	0,820	**0,941**
		R2	0,224	0,272	0,218	0,144	0,196	0,206	0,070	0,183	0,177	0,152	0,184
dB4	1	R1	1	1	1	1	0,963	0,990	0,854	1	0,984	0,899	**0,969**
		R2	0,188	0,249	0,178	0,193	0,222	0,237	0,081	0,211	0,218	0,190	0,197
	2	R1	1	1	1	1	1	1	1	1	1	0,964	**0,996**
		R2	0,225	0,280	0,232	0,238	0,234	0,301	0,209	0,222	0,241	0,250	0,243
	3	R1	0,944	1	1	1	1	1	0,993	1	1	0,964	**0,990**
		R2	0,208	0,295	0,210	0,213	0,257	0,353	0,198	0,229	0,250	0,253	0,247
dB5	1	R1	1	1	1	1	1	0,991	0,861	1	0,992	0,958	**0,987**
		R2	0,194	0,259	0,185	0,202	0,207	0,265	0,128	0,064	0,216	0,202	0,192
	2	R1	0,981	0,991	1	1	0,927	0,991	0,876	1	0,976	0,892	**0,963**
		R2	0,166	0,234	0,159	0,161	0,199	0,210	0,071	0,198	0,189	0,155	0,174
	3	R1	0,981	0,991	1	1	1	0,991	0,891	1	0,976	0,942	**0,977**
		R2	0,164	0,230	0,157	0,160	0,187	0,211	0,065	0,197	0,188	0,130	0,169
dB6	1	R1	1	1	1	1	1	1	0,898	1	1	0,957	**0,986**
		R2	0,227	0,268	0,220	0,257	0,248	0,296	0,151	0,221	0,269	0,216	0,237
	2	R1	0,953	0,991	1	1	0,872	0,991	0,876	1	0,976	0,871	**0,953**
		R2	0,159	0,255	0,150	0,171	0,206	0,210	0,068	0,191	0,183	0,144	0,171
	3	R1	0,944	0,981	1	0,904	,0963	0,972	0,876	0,947	0,952	0,914	**0,945**
		R2	0,134	0,269	0,123	0,124	0,172	0,219	0,062	0,185	0,122	0,158	0,140
dB7	1	R1	0,963	1	1	1	0,950	0,991	0,861	1	0,968	0,914	**0,965**
		R2	0,213	0,259	0,182	0,184	0,225	0,237	0,083	0,203	0,224	0,189	0,200
	2	R1	0,958	0,991	1	1	0,908	0,991	0,836	1	0,968	0,827	**0,948**
		R2	0,173	0,239	0,164	0,204	0,224	0,225	0,079	0,204	0,209	0,184	0,191
	3	R1	0,963	1	1	1	1	0,991	0,869	1	0,976	0,950	**0,975**
		R2	0,185	0,257	0,176	0,178	0,206	0,233	0,069	0,200	0,218	0,154	0,188
dB8	1	R1	0,981	0,991	1	1	0,890	0,991	0,854	0958	0,968	0,827	**0,946**
		R2	0,159	0,219	0,150	0,145	0,196	0,206	0,072	0,183	0,178	0,152	0,166
	2	R1	0,958	0,991	1	1	0,917	0,991	0,869	1	0,992	0,799	**0,954**
		R2	0,190	0,252	0,205	0,218	0,245	0,259	0,089	0,212	0,224	0,208	0,210
	3	R1	0,981	0,991	1	1	0,890	0,991	0,876	0,958	0,976	0,899	**0,956**
		R2	0,128	0,219	0,150	,0144	0,196	0,206	0,068	0,183	0,177	0,114	0,162

In Table 4.2 some of the Daubechies wavelets from dB3 to dB8 were used. Our wavelet has more performance than Daubechies wavelet except dB4 wavelet. Its performance is 99,6% where our wavelet has a 99,3% performance.

Table 4.3.Experimental results with Symlet wavelets.

			Ratio of Detected R Peaks										
Approaches \ ECGs			1	2	3	4	5	6	7	8	9	10	**Success**
SYM3	1	R1	1	1	1	1	1	1	0,854	1	1	0,992	**0,984**
		R2	0,223	0,263	0,218	0,241	0,243	0,287	0,149	0,213	0,262	0,200	0,230
	2	R1	1	1	1	1	1	1	0,905	1	1	0,992	**0,990**
		R2	0,225	0,262	0,217	0,254	0,256	0,294	0,112	0,226	0,274	0,206	0,233
	3	R1	1	1	1	1	1	1	0,905	1	1	0,971	**0,988**
		R2	0,224	0,272	0,217	0,254	0,256	0,294	0,112	0,226	0,274	0,206	0,234
SYM4	1	R1	1	1	1	0,981	0,982	0,981	0,883	1	0,976	0,978	**0,978**
		R2	0,154	0,150	0,175	0,222	0,231	0,248	0,071	0,213	0,224	0,166	0,185
	2	R1	1	1	1	1	1	0,990	0,890	1	0,984	0,986	**0,986**
		R2	0,198	0,220	0,191	0,211	0,223	0,256	0,078	0,215	0,232	0,182	0,200
	3	R1	0,981	1	1	1	1	0,990	0,890	1	0,984	0,986	**0,983**
		R2	0,184	0,256	0,174	0,183	0,205	0,241	0,073	0,200	0,214	0,155	0,189
SYM5	1	R1	0,981	0,981	1	1	1	0,990	0,839	0,978	0,986	0,986	**0,990**
		R2	0,154	0,210	0,147	0,148	0,173	0,194	0,061	0,179	0,171	0,124	0,156
	2	R1	0,981	1	1	1	1	0,990	0,905	1	1	0,985	**0,986**
		R2	0,199	0,254	0,187	0,226	0,228	0,252	0,083	0,213	0,230	0,190	0,206
	3	R1	0,981	1	1	1	1	0,990	0,883	1	0,984	0,978	**0,981**
		R2	0,179	0,246	0,173	0,205	0,215	0,196	0,071	0,207	0,218	0,163	0,187

In Table 4.3 results obtained by using some Symlet wavelets are shown. Symlets wavelets provide close but lower success than our wavelet.

Table 4.4.Experimental results with Coiflet wavelets.

			Ratio of Detected R Peaks										
ECGs / Approaches			**1**	**2**	**3**	**4**	**5**	**6**	**7**	**8**	**9**	**10**	**Success**
COIF3	1	R1	0,981	0,991	1	1	0,992	0,991	0,883	1	0,976	0,978	**0,979**
		R2	0,181	0,245	0,171	0,214	0,221	0,239	0,071	0,211	0,215	0,165	0,193
	2	R1	1	1	1	1	1	1	0,891	1	0,984	0,986	**0,986**
		R2	0,196	0,252	0,181	0,223	0,229	0,254	0,076	0,213	0,230	0,182	0,203
	3	R1	0,981	0,991	1	1	0,992	0,991	0,883	1	0,976	0,978	**0,979**
		R2	0,181	0,245	0,171	0,214	0,221	0,239	0,071	0,211	0,215	0,165	0,193
COIF 4	1	R1	1	1	1	1	1	0,992	0,898	1	0,992	0,986	**0,987**
		R2	0,202	0,255	0,189	0,230	0,233	0,265	0,084	0,211	0,241	0,190	0,210
	2	R1	1	1	1	1	1	1	0,905	1	0,992	0,986	**0,988**
		R2	0,202	0,255	0,188	0,230	0,233	0,265	0,084	0,211	0,241	0,190	0,215
	3	R1	1	1	1	1	1	0,992	0,898	1	0,992	0,986	**0,987**
		R2	0,202	0,255	0,189	0,230	0,233	0,265	0,084	0,211	0,241	0,190	0,210
COIF 5	1	R1	1	1	1	1	1	1	0,891	1	0,982	0,987	**0,987**
		R2	0,199	0,255	0,189	0,230	0,230	0,258	0,080	0,207	0,237	0,188	0,184
	2	R1	0,981	1	1	1	1	1	0,891	1	0,988	0,978	**0,984**
		R2	0,187	0,246	0,174	0,236	0,242	0,268	0,075	0,216	0,229	0,175	0,205
	3	R1	1	1	1	1	1	1	0,891	1	0,982	0,987	**0,987**
		R2	0,199	0,255	0,189	0,230	0,230	0,258	0,080	0,207	0,237	0,188	0,184

Table 4.5.Experimental results with Meyer wavelet.

			Ratio of Detected R Peaks										
ECGs / Approaches			1	2	3	4	5	6	7	8	9	10	Success
MEYER	1	R1	0,944	0,925	1	1	0,800	0,990	0,846	0,915	0,952	0,719	**0,909**
		R2	0,134	0,185	0,129	0,128	0,166	0,175	0,065	0,157	0,142	0,124	0,141
	2	R1	0,944	0,953	1	1	0,780	0,935	0,832	0,915	0,952	0,748	**0,906**
		R2	0,135	0,197	0,129	0,147	0,196	0,197	0,067	0,168	0,151	0,139	0,153
	3	R1	0,944	0,925	1	1	0,770	0,935	0,839	0,915	0,952	0,777	**0,906**
		R2	0,133	0,185	0,129	0,190	0,169	0,178	0,065	0,158	0,143	0,124	0,147

In Table 4.4 and Table 4.5, results obtained by using some of the Coiflet wavelets and Meyer wavelet are shown. We can easily comment that coiflet wavelets have lower but close performance to our wavelet. The performance of Meyer wavelet is the worst.

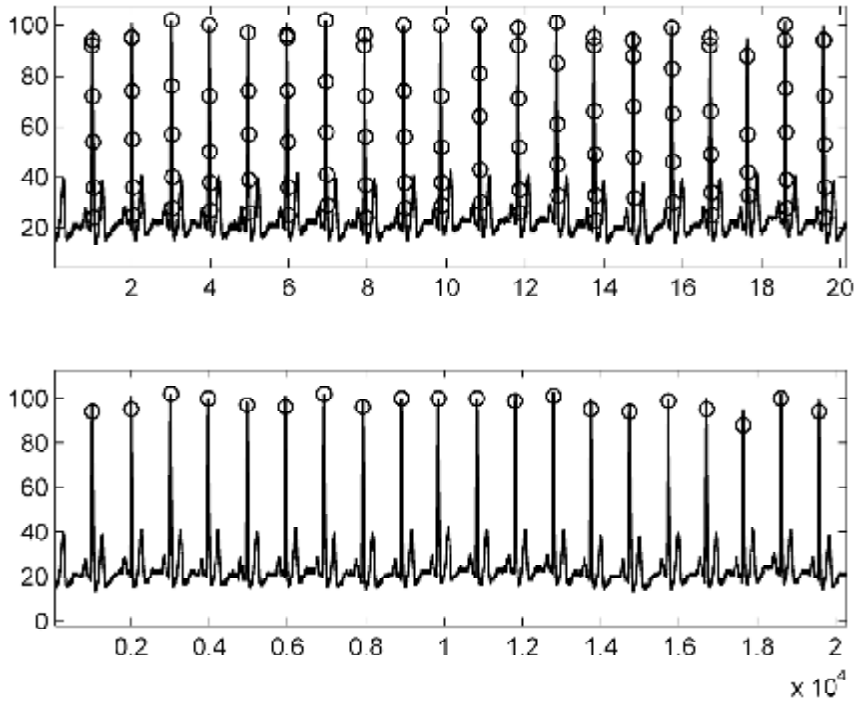

Figure 4.19.QRS detection before and after post-processing. Approximations coefficients of custom wavelet are used for determining threshold level.

In Figures 4.21 a sample ECG signal before and after the post processing stage are shown. The detected R peaks marked on the graphics. As mentioned before, the R2 coefficients in Tables 4.1, 4.2, 4.3, 4.4, 4.5 show that our post processing procedure eliminates the false R peaks effectively.

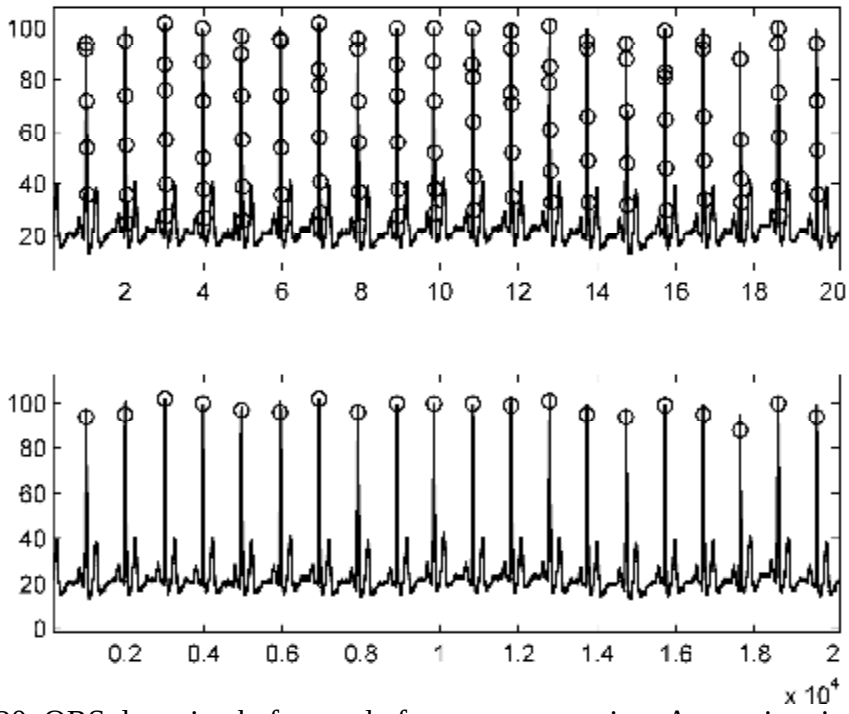

Figure 4.20. QRS detection before and after post-processing. Approximations coefficients of dB4 wavelet are used for determining threshold level.

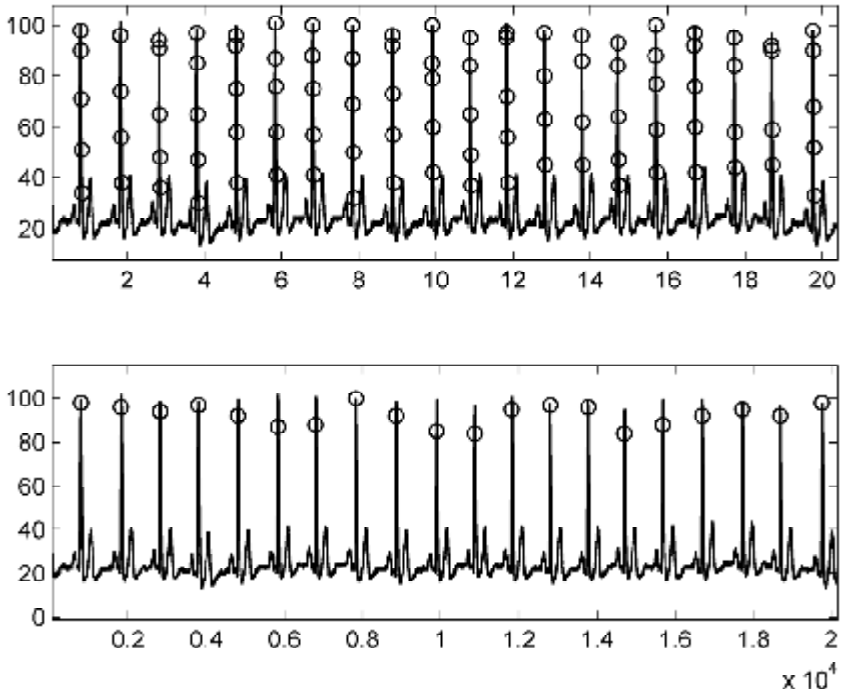

Figure 4.21. QRS detection before and after post-processing. Approximations coefficients of Sym3 wavelet are used for determining threshold level.

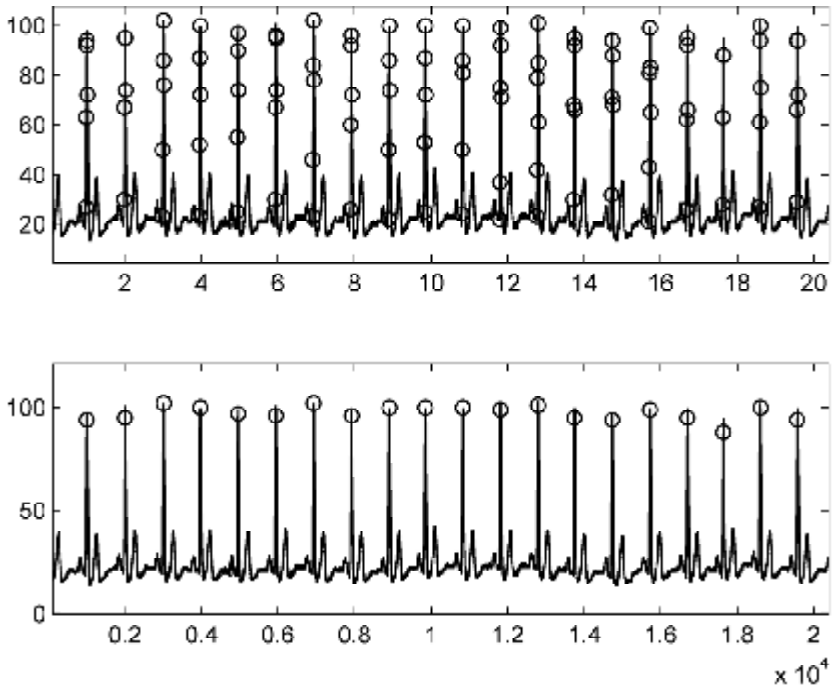

Figure 4.22. QRS detection before and after post-processing. Approximations coefficients of Coiflet4 wavelet are used for determining threshold level.

In Figures 4.22, 4.23 and 4.24 the graphical representation of QRS detection before and after post processing are shown with using dB4, Sym3 and Coif5 wavelets respectively.

Table 4.6. Experimental results obtained by employing DWT.

			Ratio of Detected R Peaks										
Approaches \ ECGs			1	2	3	4	5	6	7	8	9	10	Success
DWT	1	R1	1	1	1	1	1	1	0,949	1	1	0,914	0,986
		R2	0,183	0,236	0,197	0,264	0,263	0,275	0,123	0,210	0,255	0,210	0,224
	2	R1	1	0,981	1	1	1	1	1	1	0,872	1	0,985
		R2	0,207	0,391	0,209	0,236	0,218	0,214	0,323	0,178	0,334	0,336	0,264
	3	R1	1	1	1	1	0,991	1	0,950	1	1	0,921	0,986
		R2	0,207	0,237	0,195	0,266	0,262	0,278	0,115	0,210	0,255	0,239	0,226

We also used DWT for QRS detection. As it is well known DWT is a fast wavelet transform. The computation of the wavelet-transform coefficients is faster with DWT. The tree depth of the wavelet-tree is chosen as J = 3. As it is seen from

Table 4.6, our wavelet provides a fairly good performance with 98.6% of R-peak detection.

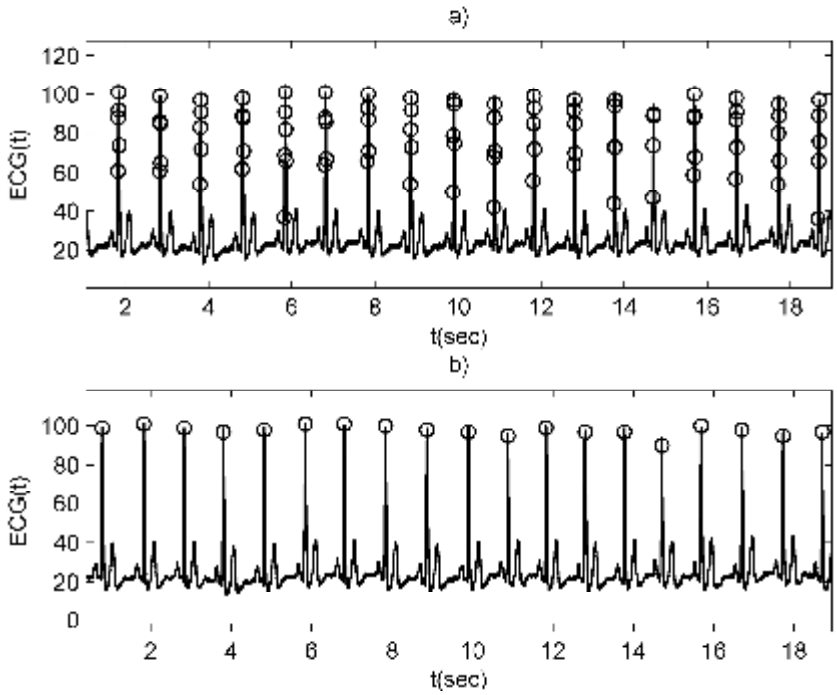

Figure 4.23.QRS Detection before and after post-processing with using custom filter by DWT method

In Figure 4.24 approximation coefficients and detail coefficients of the ECG signal with DWT with J=3 is shown. We used the custom filters for filtering. These wavelet coefficients were used for QRS detection and as it is seen from Table 4.6, a satisfactory performance is obtained.

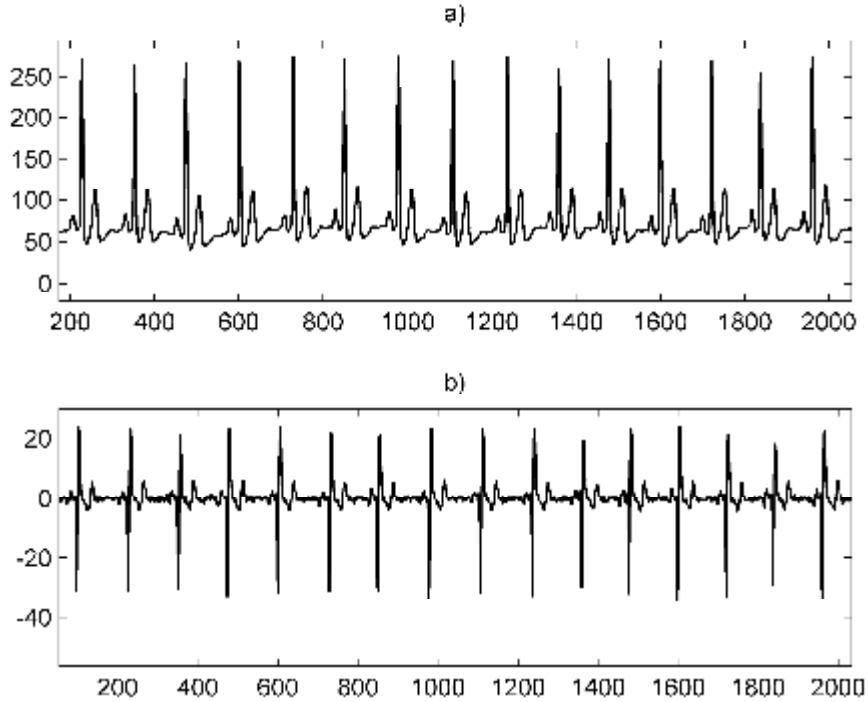

Figure 4.24. a) Approximation coefficients of an ECG signal at level 3 with using custom filter by DWT method
b) Detail coefficients of an ECG signal at level 3 with using custom filter by DWT method

The relation between custom filters and the filters of the wavelets that used in this thesis is analyzed statistically by using correlation coefficients. First we compared the filter length of our wavelet with the filter length of common wavelet that we used separately. Then we extended the short filter by adding zeros. The cross correlation coefficients were computed by estimating the cross correlation sequences of the custom wavelet with some common wavelets. The highest value of this sequence is used to compute the standard deviation. This process gave us the closeness relation. Table 4.7 shows the correlation coefficients between custom wavelet and other wavelets. As the correlation coefficient come closer to 1, the correlation level increases and this means that the filters are more similar to each other. When we investigate this table we find that custom wavelet is more similar to dB5, dB4 and Symlet5 wavelets. The correlation for Coiflet3, Coiflet4, Coiflet5, Symlet4 and Meyer are nearly at same level and have a lower correlation coefficient than dB4, dB5 and Sym5 wavelets.

Table 4.7.Correlation coefficients between custom wavelet and some knowing wavelets.

		Low Pass Filters				High Pass Filters	
		Coefficients	Lags			Coefficients	Lags
Wavelets	dB3	0.8288	11	Wavelets	dB3	0.8621	14
	dB4	**0.9273**	10		dB4	**0.9516**	14
	dB5	**0.9474**	8		dB5	**0.9516**	14
	dB6	0.9059	6		dB6	0.9236	14
	dB7	0.8232	5		dB7	0.8442	13
	dB8	0.8962	3		dB8	0.9086	13
	Sym3	0.8288	11		Sym3	0.8621	14
	Sym4	0.8535	13		Sym4	0.8884	11
	Sym5	**0.9263**	11		Sym5	**0.9527**	11
	Coif3	0.8644	4		Coif3	0.8807	10
	Coif4	0.8689	0		Coif4	0.8771	8
	Coif5	0.8573	-4		Coif5	0.8742	6
	Meyer	0.8515	-36		Meyer	0.8613	-34

The highest correlations are in term obtained with db5, db4 and Sym5 (Table 4.7). These outcomes coincide with the R-peak detection performances. For visual comparision, the most similar low pass and high pass filters are shown in Figure 4.25 and Figure 4.26.

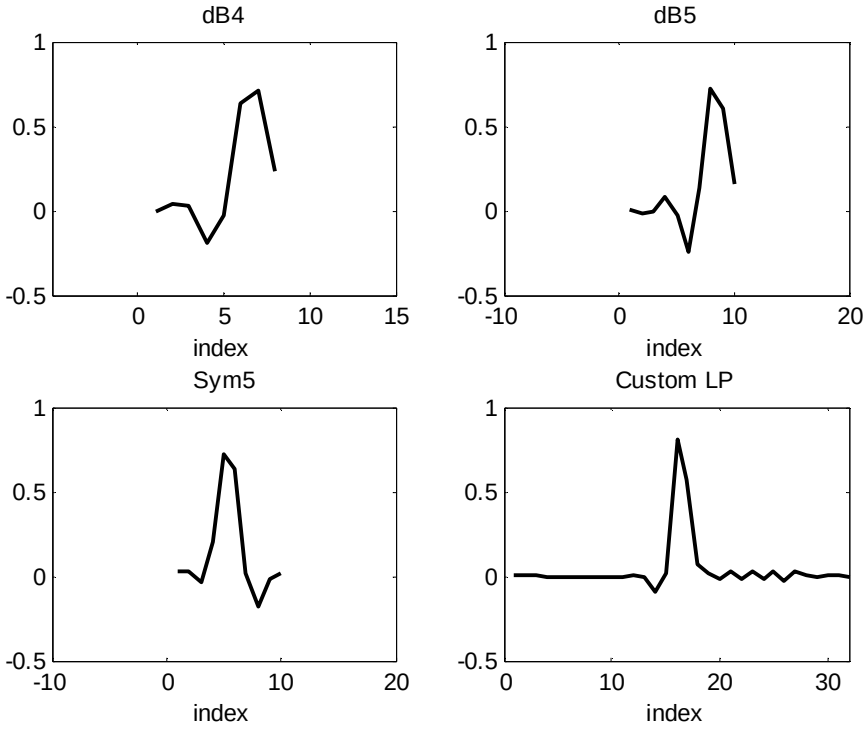

Figure 4.25.Low Pass Filters of some known wavelets and custom wavelet

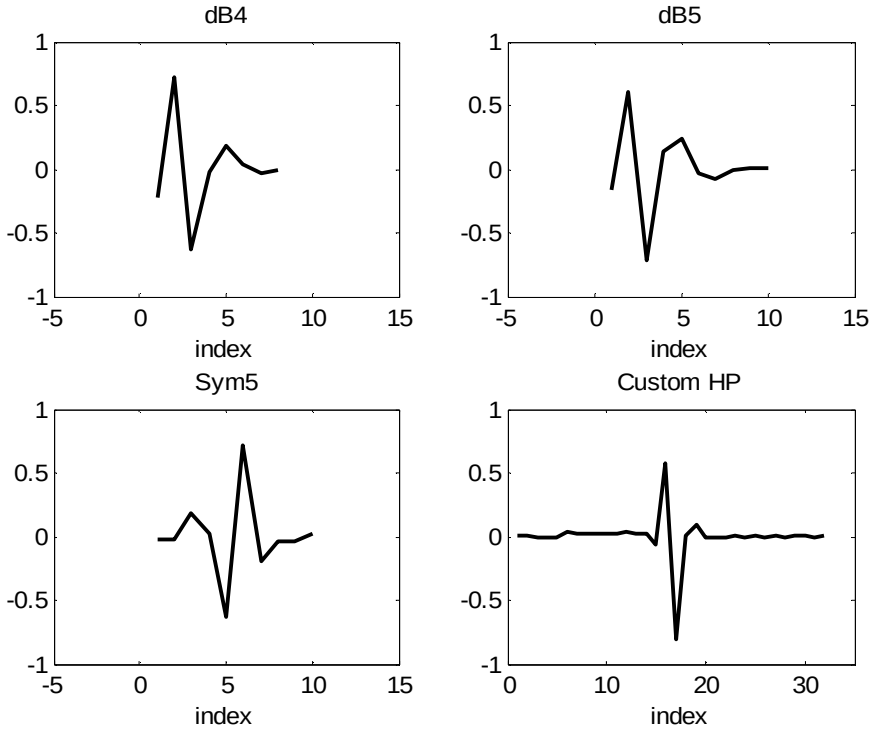

Figure 4.26.High Pass Filters of some known wavelets and custom wavelet

When we compare visually the Figure 4.25 and 4.26, the similarity between custom wavelet and dB4, dB5 and Sym5 wavelets can be easily seen and that supports the results in Table 4.7.

5. RESULTS AND SUGGESTIONS

In this thesis, we detected R-peaks in an ECG signal by using wavelet decomposition. We also constructed an orthogonal multi-resolution system with a scaling function resembling the shape of the R-wave which promises a good performance in detecting R-peaks and hence QRS wave. To obtain the custom system we first determined a function resembling an R peak to construct the scaling function. The advantage of our system is based on this scaling function because it contains the characteristic properties of the QRS complex. This function has been orthogonalized and its wavelet counterpart has been obtained. The low pass and high pass FIR filters are obtained from dilation and two-scale equations respectively. The low pass and high pass filters are tuned to present the orthogonality.

ECG signal lies between 1 Hz and 40 Hz and since the sampling frequency is 1000 Hz, this band is covered at the third scale of wavelet decomposition. Hence, approximation and detail coefficients of third scale are computed. Besides these coefficients, square root of sum of the squares of the coefficients is also employed for R-peak identification. By using overlapping windows, the ECG is segmented and each segment is decomposed by the discrete wavelet transform up to level three.

A threshold was decided from the wavelet coefficient of the initial 30 seconds data eliminate the coefficients which are related to QRS complexes. Overlapping windows causes many false R-peak detection and this problem is solved by post processing the results; the neighbor R-peaks are compared if there time indices are less than 6 the one with lower absolute value is eliminated.

The computer used for implementing the algorithm was equipped with an i5 microprocessor with a 2.8GHz clock frequency and 4 GB DDR3 RAM. The algorithm took approximately 3 minutes to detect R-peaks by using continuous wavelet transform. The time needed to run algorithm was about 3 seconds when discrete wavelet transform is chosen. Due to its fast implementation, the DWT method is preferred in clinical medicine.

Beside the custom wavelet, the algorithm is also run for well-known wavelet families; Daubechies, Symlet, Coiflet and Meyer. The result obtained by wavelet is

satisfactory; 99% of the R-peaks are detected accurately as shown in the Table 4.1. very close results are obtained especially with dB4, dB5 and Sym5 wavelets; they are given in Table 4.2, 4.3 and 4.4. As one expected the outcomes do not change when DWT is employed. In general magnitude coefficients provided better results than using approximation and detail coefficients.

The correlation between custom wavelet and the common wavelets was computed to find reasoning about performances of the wavelets. When the computed correlation-coefficients are investigated it is seen that custom wavelet is quite similar to dB4, dB5 and Sym5 wavelets in terms of shape. This explains why the success of these wavelets is very close to the success of the custom wavelet.

Kumari et al (2007) in their study design orthogonal low pass and high pass filters directly by using parameterized perfectly reconstruction They design many filters by changing the parameter use the designed filters to remove noise from ECG. Apart from this approach, in this study our algorithm is based on specifying the basis function. Our basis function is derived from a function that resembling the R-wave. So it contains the characteristics of the R peaks and it provides strong resemblance index. Scaling function and its complementary wavelet are specified and corresponding low pass and high pass filters are extracted. This index is the compact wavelet coefficients of the ECG signal and the R-peaks are determined from these wavelet coefficients.

When the results of the study are compared with other QRS detectors in the literature, it is impossible to reach an accurate conclusion because ECG signals used in these studies are different.

The performance of the algorithm shows that it is reliable and successfully used for R-peak and/or QRS detection provided that the algorithm have been tested with much bigger and different databases to support and improve the credibility of the results of this study.

REFERENCES

ABIBULLAEV B., SEO H.D., 2011, A New QRS Detection Method Using Wavelets and Artificial Neural Networks, J Med Syst. (35), 683–691.

ADDISON P.S., 2002, Illustrated Wavelet Transform Handbook, Introductory Theory and Applications in Science, Engineering, Medicine and Finance, Taylor & Francis, p400.

AKANSU A.N., HADDAD R.A., 2001, Multiresolution Signal Decomposition: Transforms, Subbands, and Wavelets, Academic Press, p499.

ALLEN R.L., MILLS D., 2004, Signal Analysis (Hardback) Time, Frequency, Scale and Structure, John Wiley and sons Ltd., p966.

ARICA S., 2007, Elektroansefalografi İşaretlerinin Çözümleme ve Bireşimi İçin Bir Dikey Ölçekleme ve Dalgacık İşlevi Çifti, IEEE SİU'07 Kurultayı

ARICA S., INCE N.F., BOZKURT A.,TEWFIK A.H., BIRAND A., 2011, Prediction Of Pharmacologically Induced Baroreflex Sensitivity From Local Time And Frequency Domain Indices Of R-R Interval and Systolic Blood Pressure Signals Obtained During Deep Breathing, Computers in Biology and Medicine, Volume 41, Issue 7, 442-448.

BENITEZ D.S., GAYDECKI P.A., ZAIDI A., FITZPATRICK A.P., 2000, A New QRS Detection Algorithm Based on the Hilbert Transform, Computers in Cardiology, 379-382.

BOUTAA M., BEREKSI-REGUIG F., DEBBAL S.M.A., 2008, ECG Signal Processing Using Multiresolution Analysis, Journal of Medical Engineering & Technology, 32:6, 466-478.

BRONZINO J.D, 2000, The Biomedical Engineering Handbook, A CRC Handbook Published in Cooperation with IEEE Press, p185.

BSOUL A.B., JI S., WARD K., NAJARIAN K., 2009, Detection of P, QRS, and T Components of ECG Using Wavelet Transformation, ICME International Conference, 1-6.

BURRUS C.S., GOPINATH R.A.,GUO H., 1997, Introduction to Wavelets and Wavelet Transforms, a Primer, Prentice Hall Inc., p268.

CASTRO B., KOGAN D., GEVA A.B., 2000, Detection of ECG Characteristic Points Using Wavelet Transform, IEEE Transactions on Biomedical Engineering, Vol. 42, No 1; 21-28.

CHAN Y.T., 1995, Wavelet Basics, Kluwer Academic Publishers, p144.

CHAWLA M.P.S., VERMA H.K., 2006, ECG Modeling and QRS Detection using Principal Component Analysis, Advances in Medical, Signal and Information Processing, 1-4.

CHOUKARI S.A., BEREKSI-REGUING F., AHMAIDI S. AND FOKAPU O., 2006, ECG Signal Smoothing Based On Combining Wavelet Denoising Levels, Asian Journal of Information Technology 5(6), 666–677.

CROMWELL L., WEIBELL F.J., PFEIFFER A., 2005, Biomedical Instrumentation and Measurements, Prentice Hall of India, New Delhi, p446.

COHEN K.P., TOMPKINS W.J., DJOHAN A, 1995, QRS Detection Using A Fuzzy Neural Network, Engineering in Medicine and Biology Society, IEEE, 17th Annual Conference 189-190.

DANIEL T.L., YAMAMOTO A., 1994, Wavelet Analysis: Theory and Applications, Hewlett Packard Journal, 44-52.

DINH H.A.N, KUMAR D.K, PAH N.D., BURTON P., 2001, Wavelets for QRS Detection, 23rd Annual Conference – IEEE/EMBS, İstanbul, 1883-1887

DAUBECHIES, I., 1992, Ten lectures on Wavelets, SIAM, Philadelphia, p377.

DAQROUQ K., ABU-ISBEIH I.N., AL-QASWASMI A.R., 2008, QRS Complex Detection Based on Symlets Wavelet Function, Systems, Signals and Devices, IEEE 5th International Multi Conference, 1-5.

DESPOPOULOS A., SILBERNAGL S., 2001, Color Atlas of Physiology, Georg Thieme Verlag, p436.

DUBOVIK K., 1999, Automated Arrhythmia Analysis-An Expert System for an Intensive Care Unit, Lund University, Sweden, Lund.

ELGENDI M., JONKMAN M., DE BOER F., 2009, R Wave Detection using Coiflets Wavelets , Proceedings IEEE, 1-4.

FRADEN J., NEUMAN M. R., 1980, QRS Wave Detection, Med. Biolog. Eng. Comput., 18, 125-132.

GANESAN R., DAS T.K., VENKATARAMAN V., 2004, Wavelet-Based Multiscale Statistical Process Monitoring: A Literature review. IIE Transactions, Volume 36, Issue 9, 787–806.

GAO R., YAN R., 2011, Wavelets- Theory and Applications for Manufacturing, Springer Science+ Business Media, London, p223

GESZTESY F., HOLDEN H., JOST J., 1999, Stochastic Processes, Physics and Geometry, Amer Mathematical Society, p333

GROSSMANN A., MORLET J., 1984, Decomposition of Hardy Functions into Square Integrable Wavelets of Constant Shape, SIAM J. Math. Anal., 15, 723-736.

HAMPTON J.R., 2003, ECG Made Easy, Churchill Livingstone, p192.

HE T. X., 2004, Biorthogonal Spline Type Wavelets. Computers Mathematics with Applications, 48(9), 1319-1334.

HERNANDEZ E., and WEISS G., 1996, A First Course on Wavelets, Boca Raton, FL: CRC Press, p489.

HOWARD N.K., 2005, Multiscale Analysis of Landscape Data Lands from northern Ghana: Wavelets and Pattern Metrics, University of Bonn, p128.

INCE N.F., ARICA S., BIRAND A., 2003, A PC Based Data Acquisition and Signal Processing System for Measuring the Baroreceptor Sensitivity, Proceedings of the IASTED International Conference on Signal Processing, Pattern Recognition, and Applications, 93-97.

JORGENSEN P.E.T., 2006, Analysis and Probability Wavelets, Signals, Fractals, Springer, p276.

KADAMBE S., MURRAY R., BOUDREAUX G.F., 1999, Wavelet Transform Based QRS Complex Detector, Biomedical Engineering, IEEE Transactions on Volume:46 Issue:7, 838-848.

KANIA M., FERENIEC M., MANIEWSKI R., 2007, Wavelet Denoising for Multi-

lead High Resolution ECG Signals, Measurement Science Review, Vol.7, Section 2, No.4, 30-33.

KAREL J.M.H., PEETERS R.L.M., WESTRA R.L., MOERMANS K.M.S., HADDAD S.A.P., and SERDIJN W.A., 2005, Optimal Discrete Wavelet Design For Cardiac Signal Processing. 27th Annual International Conference of the IEEE Engineering In Medicine And Biology Society, 2769–2772.

KARPAGACHELVI S., ARTHANARI M., SIVAKUMAR M., 2010, QRS Wave Detection Using Multiresolution Analysis, Vol. 10 Issue 5 Ver. 1.0, 39-42.

KOZAKEVICIUS A., RODRIGUES C., NUNES R.C., FILHO R.G., 1988, Adaptive ECG Filtering and QRS Detection Using Orthogonal Wavelet Transform, Engineering in Medicine and Biology Society, Proceedings of the Annual International Conference of the IEEE vol.1: 1147-1148.

KTATA S., OUNI K., ELLOUZE N., 2006, ECG Signal Maxima Detection Using Wavelet Transform, IEEE ISIE, 700-703.

KUMARI R.S., BHARATHI S., SADASIVAM V., 2007, Design of Optimal Discrete Wavelet for ECG Signal Using Orthogonal Filter Bank, International Congress on Computational Intelligence and Multimedia Applications, 525

LEGARRETA I., ADDISON P.S., REED M.J., GRUBB N.R., CLEGG G.R., ROBERTSON C.E. and WATSON J.N., 2005, Continuous Wavelet Transform Modulus Maxima Analysis of the Electrocardiogram: Beat-to-beat Characterization and Beat to- Beat Measurement Int. J. Wavelets, Multiresolution Inf. Process. 3: 19–42.

LI C.W., ZHENG C.X., TAI C.F., 1995, Detection of ECG Characteristic Points Using Wavelet Transforms, IEEE Trans. Biomed. Eng. 42 (1): 21–28

MALLAT, S., 1989, Multiresolution Approximations and Wavelet Orthogonormal Bases of $L^2(R)$, Trans. Amer, Math. Soc., 315: 69-87.

MALLAT S., 1999, A Wavelet Tour of Signal Processing, Academic Pres, p620.

McDARBY G., CELLER B.G, LOVELL N.H., 1998, Characterizing the Discrete Wavelet Transform of an ECG Signal with Simple Parameters for use in Automated Diagnosis, 2nd International Conference on Bioelectromagnetism, Melbourne, 31-32.

MERTINS A., 1999, Signal Analysis: Wavelets, Filter Banks, Time-Frequency Transforms and Applications, John Wiley and Sons, West Sussex England, p330

MESSAOUD M.B., KHELIL B., KACHOURI A., 2009, Analysis and Parameter Extraction of P Wave Using Correlation Method, The International Arab Journal of Information Technology, Vol. 6, No. 1, 40-46.

NICK K., JULIAN M., 1997, Wavelet Transform in Image Processing. Signal Processing and Prediction I, Eurasip, ICT press, 23-34.

NOVA'K D., 2000, Processing Of ECG Signal Using Wavelets, Master Thesis, Czech Technical University in Prague.

OLIVERIA I.F., CORTEZ P.C., 2004, A QRS Detection Based on Hilbert Transform and Wavelet Bases, IEEE workshop on Machine Learning for Signal Processing, 481-489.

PLONKA G., SCHUMACHER H., TASCHE M., 2008, Numerical Stability of Biorthogonal Wavelet Transforms, Advances in Computational Mathematics, Volume 29, Number 1, 1-25.

PORTOLES L.B., 2009, Lossless Compression of ECG signals, Performance Analysis in a Wireless Network.

QIU Y.Z., DING X.F., FENG J., 2006, QRS Complexes Detection Based On Mexican-Hat Wavelet, Journal of Biomedical Engineering, 23(6), 1347-1349.

RAGHUVEER M.R., BOPARDIKAR S., 1998, Wavelet Transforms, Introduction to Theory and Applications, Prentice Hall PTR, p310.

RIZZI M., ALOIAASTAGNOLO M.D., 2008, Fast Parallelized Algorithm for ECG Analysis, WSEAS Transaction on Biology and Medicine, Issue 8, vol.5.

RUHA A., SALLINEN S., NISSILIA S., 1997, A Real-Time Microprocessor QRS Detector System with a 1ms Timing Accuracy for Measurement Of Ambulatory HRV, Transactions on Biomedical Engineering, 44(3):159-167.

SAHAMBI J.S., TANDON S.M., BHATT R.K.P., 1997, Using Wavelet Transforms For ECG Characterization: an On-line Digital Signal Processing System, IEEE ENG. Med. Biol. 16: 77–83.

SASIKALA P., WAHIDABANU R.S.D, 2010, Robust R peak and QRS Detection in Electrocardiogram using Wavelet Transform, International Journal of Advanced Computer Science and Application, 1(6), 48-53.

SARITHA C., SUKANYA V., MURTHY Y.N., 2008, ECG Signal Analysis Using Wavelet Transforms, Bulg. J. Phys. 35, 68–77.

SEMMLOV J.L., 2004, Biosignal and Biomedical Image Processing MATLAB Based Applications, CRC Pres, p448.

SHENG, Y., 2000, Wavelet Transform, The Transforms and Applications Handbook: Third Edition, CRC Pres., p911.

SINGH B.N., TIWARI A.K., 2006 Optimal Selection of Wavelet Basis Function Applied to ECG Signal Denoising, Digital Signal Processing, Volume 16, Issue 3, 275-287.

SOMAN K.P., RAMACHANDRAN K.I., 2008, Insight into Wavelets From Theory to Practice, Prentice-Hall, p404.

STRANG G., NGUYEN T., 1996, Wavelets and Filter Banks, Wellesley-Cambridge Pres, p520.

SZILAGYI L., 2001, On-Line QRS Complex Detection Using Wavelet Filtering, Engineering in Medicine and Biology Society, Proceedings of the 23rd Annual International Conference of the IEEE, Volume: 2, 1872-1874.

SZILAGYI S.M., SZILAGYI L., 2000, Wavelet Transform and Neural Network Based Adaptive Filtering for QRS Detection, Proceedings of the 22th Ann. EMBS Int.Conf., 1267-1270.

TAN K.F., 2000, Detection of the QRS complex, P wave and T wave in Electrocardiogram, Advances in Medical Signal and Information Processing, 2000. First International Conference on (IEE Conf. Publ. No. 476), 41-47.

TEOLIS A.,1998, Computational Signal Processing with Wavelets, Birkhauser, Boston, MA., p348.

TIKKANEN P., 1999, Characterization and Application Of Analysis Methods For ECG and Time Interval Variability Data. PhD Thesis, University of Oulu, Finland.

TOMPKINS W,J., PAN J., 1995, A Real-Time QRS Detection Algorithm, IEEE Transaction on Biomedical Eng. BME-32. No.3. 230-235.

VETTERLI, M., HERLEY, C., 1992, Wavelets and Filter Banks: Theory and Design. IEEE Trans. Acoust. Speech Signal Process., 40(9), 2207-2232.

VIJAYA G., KUMOR V., VERMA H.K., 1997, Artificial Neural Network Based Wave Complex Detection in Electrocardiograms, Int. Journal of System Science, 125-132.

ZHANG W., GE L., 2008, Application of Adaptive Matched Filter to ECG Signal Detection, Proceedings of the 7th World Congress on Intelligent Control and Automation, 7960-7964.

ZHOU S.K., WANG T.J., XU R., 1988, The Real-time Detection of QRS Complex using the Envelope of ECG, proc. 10th Annu. Int. Conf., p38

WALKER J.S., 2008, A Primer on Wavelets and Their Scientific Applications Second Edition, Chapman&Hall/CRC, p168.

RESUME

Cem Sakarya was born in Niğde in 1970. He received BSc. Degree in Electronics Engineering Department from Erciyes University, Kayseri in 1995. He worked as an Electronics Engineer at different companies for nearly 2 years. Now he has been working as a lecturer for 14 years in Nigde University.

APPENDIX

Matlab Code

```
clear all
close all
ecg = load('ECG_1.dat');
% 30 SECOND OF THE ECG SIGNAL
M = 30000;
fs = 1000;
x = ecg(1:M);
h = fir1(20, 0.1);
x = conv(x, h);
x = x(11:M+10);
ts = 0.001; % sampling interval
t = (0 : M-1) * ts;
% ECG signal
plot(t, x);
%D is drift
D=10;
%W is the length of the window
W=100;
y= extractseg(x, D, W, []);
%phio is orthogonolized scaling function
[L, N] = size(y);
%finding approximation coefficients
ak = akcoeff(y);
% threshold level
aksort=sort(abs(ak));
lak=length(aksort);
aksort=aksort(1/3*lak:end);
th=mean(aksort);
akn=find(abs(ak)>th);
```

```
ak2=ak(akn);
%eliminating 1/3 of the lowest part of approximation coefficients
%calculating the new threshold level by feedback
aksort=sort(abs(ak2));
lak=length(aksort);
aksort=aksort(1/3*lak:end);
th=mean(abs(aksort));
%c is the class
clear y ak
y= extractseg(ecg, D, W, []);
%phio is orthogonolized scaling function
ak = akcoeff(y);
c=abs(ak)>th;
q=find(c==1);%qrs
k=(q-1)*D+floor(W/2);%time index
x=ecg;
n = length(x);
t = (0 : n-1) * ts;
figure(2);title('QRS DETECTION BEFORE POST PROCESSING')
subplot(2,1,1);plot(t, x, t(k), x(k), 'o');axis tight
%POST PROCESSING
qn = postprocess(ecg, q, W, D);
n = length(ecg);
t = (0 : n-1) * ts;
%figure(3); title('QRS DETECTION AFTER POST PROCESSING')
subplot(2,1,2);plot(t, ecg, t(qn), ecg(qn), 'o')
g = ((qn-1)*D)+round(W/2);
plot(g,ecg(g),'s')
hold on
plot(ecg)
%Windowing Stage
```

```
function yi = extractseg(x, D, W, m)
% x is the signal. It is a column vector.
% yi is LxN matrix. L segment length and N is segment index
L = length(x);
K = floor((L - W)/D);
x = x(1:K* D + W);
if isempty(m)
   samples = zeros(K* W, 1);
   for  k = 0 : K-1;
      samples(k*W+1: k*W + W) = x(k*D+1: k*D + W );
      yi = reshape(samples, W, K);
   end
elseif m > -1
   yi = x(m*D+1: m*D + W );
else
   yi = [];
   disp('m must be a positive integer.');
end

%Computing the approximation coefficients
function ak = akcoeff(y)
% y is AxB matrix. A segment length and B is segment index
J = 3; % 2^3 is a higher resolution from 2^0=1
[A, B] = size(y);
ts = 0.001; % sampling interval
to = 0.5;
tm = (-floor((A-1)/2):ceil((A-1)/2))*ts + to;
 p = 2^(J/2)*phio3(2^J*tm);
z = y.';
ak = zeros(1, B);
for k = 1 : B
```

```
    ak(k) = sum(z(k, :) .* p)*ts;
end
%Constructing the scaling function and wavelet function pair
function swpaira
close all
clear all
clc
a = 3;
u = @(t) (1 + sign(t))/2;
phi = @(t) a^2*t.*exp(-a*t).*u(t);
Phi = @(omega) a^(2) * 1./(1i*omega + a).^2;
M = @(omega) a^(4)*1./(omega.^2 + a.^2).^2;
b = @(omega) M(omega + 8*pi) + M(omega + 6*pi) + M(omega + 4*pi) +
M(omega + 2*pi) + ...
    M(omega) + M(omega - 2*pi) + M(omega - 4*pi) + M(omega - 6*pi) + M(omega
- 8*pi);
K = @(omega) b(omega).^(-1);
t = linspace(-6, 6, 1000);
omega  =  linspace(-5*pi, 5*pi, 1000);
figure(1); plot(t, phi(t)); title('scaling fuction');
figure(2); plot(omega, abs(Phi(omega))); title('Phi(omega)');axis tight
figure(3); plot(omega, M(omega));title('M(omega)'); axis tight
figure(4); plot(omega, b(omega).^(-1/2));title('b(omega) ^ (-1/2)'); axis tight;
figure(5); plot(omega, b(omega).^(-1));title(('1/b(omega)')); axis tight;
% Orthogonalization
po = zeros(25,1);       % -12 ... 12 (25).
for k = -12:12
    f = @(omega) (b(omega)).^(-1/2).*cos(omega*k);
    po(k+13) = 1/pi*quad(f, 0, pi);
end
```

```
phio = @(t) po(1)*phi(t+12) + po(2)*phi(t+11) + po(3)*phi(t+10) + po(4)*phi(t+9)
+ ...
   po(5)*phi(t+8) + po(6)*phi(t+7) + po(7)*phi(t+6) + po(8)*phi(t+5) +
po(9)*phi(t+4) + ...
   po(10)*phi(t+3) + po(11)*phi(t+2) + po(12)*phi(t+1) + po(13)*phi(t) + ...
   po(14)*phi(t-1) + po(15)*phi(t-2) + po(16)*phi(t-3) + po(17)*phi(t-4) +
po(18)*phi(t-5) + ...
   po(19)*phi(t-6) + po(20)*phi(t-7) + po(21)*phi(t-8) + po(22)*phi(t-9) +
po(23)*phi(t-10) + ...
   po(24)*phi(t-11) + po(25)*phi(t-12);
t = linspace(-6, 6, 1000);
n = -12:12;
figure; plot(t, phi(t)); set(gcf, 'NumberTitle', 'off', 'Name', 'Scaling Function'); axis
tight
figure; plot(t, phio(t)); set(gcf, 'NumberTitle', 'off', 'Name', 'Orthogonalized Scaling
Function'); axis tight
figure; stem(n, po, 'fill');
% Filters
omega = linspace(-2*pi, 2*pi, 1000);
figure; plot(omega, M(omega)); set(gcf, 'NumberTitle', 'off', 'Name', 'M(omega)');
axis tight
figure; plot(omega, b(omega)); set(gcf, 'NumberTitle', 'off', 'Name', 'b(omega)'); axis
tight
figure; plot(omega, b(omega)./b(2*omega)); set(gcf, 'NumberTitle', 'off', 'Name',
'b(omega)/b(2*omega)'); axis tight
clear omega
m = 12;
p = zeros(2*m+1,1);     % -m ... m (2*m+1) -> -12 ... 12 (25)
for k = -m:m
   f = @(omega) (b(omega)./b(2*omega)).^(1/2).*cos(omega*k);
   p(k+m+1) = 1/pi*quad(f, 0, pi);
```

```
end
clear t omega
n = 12;
s = quad(phi, 0, 7);
y = zeros(n+2, 1);
for k = 0:n-1
   f = @(t) phi(t) .* phi(2*t-k);
   y(k+1) = 2*quad(f, 0, 7);
end
y(n+1) = 2;
b = zeros(n, 1);
for k = 0:n-1
   f = @(t) phi(2*t) .* phi(2*t-k);
   b(k+1) = 2*quad(f, 0, 7);
end

A = [b(1)  b(2)  b(3) b(4) b(5) b(6) b(7) b(8) b(9) b(10) b(11) b(12) 1  1; b(2)  b(1)
b(2)  b(3) b(4) b(5) b(6) b(7) b(8) b(9) b(10) b(11) 1  -1;
    b(3)  b(2)  b(1) b(2) b(3) b(4) b(5) b(6) b(7) b(8)  b(9)  b(10) 1  1; b(4)  b(3)  b(2)
b(1) b(2) b(3) b(4) b(5) b(6) b(7) b(8)  b(9)  1  -1;
    b(5)  b(4)  b(3) b(2) b(1) b(2) b(3) b(4) b(5) b(6)  b(7)  b(8)  1  1; b(6)  b(5)  b(4)
b(3) b(2) b(1) b(2) b(3) b(4) b(5) b(6)  b(7)  1  -1;
    b(7)  b(6)  b(5) b(4) b(3) b(2) b(1) b(2) b(3) b(4)  b(5)  b(6)  1  1; b(8)  b(7)  b(6)
b(5) b(4) b(3) b(2) b(1) b(2) b(3) b(4)  b(5)  1  -1;
    b(9)  b(8)  b(7) b(6) b(5) b(4) b(3) b(2) b(1) b(2)  b(3)  b(4)  1  1; b(10) b(9)  b(8)
b(7) b(6) b(5) b(4) b(3) b(2) b(1) b(2)  b(3)  1  -1;
    b(11) b(10) b(9) b(8) b(7) b(6) b(5) b(4) b(3) b(2)  b(1)  b(2)  1  1; b(12) b(11)
b(10) b(9) b(8) b(7) b(6) b(5) b(4) b(3) b(2)  b(1)  1  -1;
    1     1    1   1   1   1   1   1   1   1    1    1   0  0;  1   -1    1   -1   1   -1   1
-1   1   -1   1   -1    0   0];
B = inv(A);
```

```
h = B*y;
h = h(1:n);
h = h / sqrt(2);              % h scaled by 1/sqrt(2) to make sum(h) = sqrt(2)
h = [zeros(12,1); h ; 0];      % -12 ... 12 (25)
ho = conv(h, p);               % -24 ... 24 (49)
ho = [ho; 0];                  % -24 ... 25 (50)
kb = -24;
ke = 25;
k = (kb:ke).';
go = (-1).^k .* ho((1-k) + ke);
ho = ho(10:41);                % -15 ... 16 (32)
go = go(10:41);
% Wavelet function of the orthogonal system
kb = -15;
ke = 16;
k = (kb:ke).';
go = (-1).^k .* ho((1-k) + ke);
go = [0; go];                  % -16 ... 16 (33)
po = [zeros(4,1); po; zeros(4, 1)]; % -16 ... 16 (33)
r = sqrt(2)*conv(po, go);          % -32 ... 32 (65). r is scaled by sqrt(2) since go was
%derived by from h scaled by 1/sqrt(2).
figure;
stem((-15:15), r); axis tight
set(gcf, 'NumberTitle', 'off', 'Name', 'Coefficients for constructing orthogonal wavelet
from desired scaling function'); axis tight
r = r(18:48);                  % -15 ... 15 (31)
s = 16;
% The orthogonal wavelet
psio = @(t) r(s-15)*phi(2*t+15)+r(s-14)*phi(2*t+14)+r(s-13)*phi(2*t+13)+r(s-
12)*phi(2*t+12)+r(s-11)*phi(2*t+11)+...
```

```
        r(s-10)*phi(2*t+10)+r(s-9)*phi(2*t+9)+r(s-8)*phi(2*t+8)+r(s-
7)*phi(2*t+7)+r(s-6)*phi(2*t+6)+...
        r(s-5)*phi(2*t+5)+r(s-4)*phi(2*t+4)+r(s-3)*phi(2*t+3)+r(s-
2)*phi(2*t+2)+r(s-1)*phi(2*t+1)+...
        r(s)*phi(2*t)+r(s+1)*phi(2*t-1)+r(s+2)*phi(2*t-2)+r(s+3)*phi(2*t-
3)+r(s+4)*phi(2*t-4)+...
        r(s+5)*phi(2*t-5)+r(s+6)*phi(2*t-6)+r(s+7)*phi(2*t-7)+r(s+8)*phi(2*t-
8)+r(s+9)*phi(2*t-9)+...
        r(s+10)*phi(2*t-10)+r(s+11)*phi(2*t-11)+r(s+12)*phi(2*t-
12)+r(s+13)*phi(2*t-13)+r(s+14)*phi(2*t-14)+...
        r(s+15)*phi(2*t-15);

% fine tuning
options = optimset('Display','iter');
[y, fval] = fsolve( @(x) pr(x), ho, options);
figure;
plot((-15:16), y, 'r', (-15:16), ho, 'b'); axis tight
set(gcf, 'NumberTitle', 'off', 'Name', 'Low pass filter'); axis tight
legend('Fine tuned','Designed');
ho = y;
kb = -15;
ke = 16;
k = (kb:ke).';
go = (-1).^k .* ho((1-k) + ke);
save ho.txt ho -ascii -double
save go.txt go -ascii -double

%Post-Processing Stage
function qn = postprocess(x, q, W, D)
q = q(:).';
dq = diff(q);
```

```
k = find(dq >5) + 1;
K = numel(k) + 1;
k = [1, k, numel(q)+1];
qn = zeros(1, K);
for m = 1:K
   disp(m)
   g = q(k(m):k(m+1)-1);
   g = ((g-1)*D)+round(W/2);
   [mx, t] = max(x(g));
   qn(m) = q(k(m)+t-1);
end

%DWT Application
clear all
close all
ecg = load('ECG_1.dat');
M = 30000;
fs = 1000;
x = ecg(1:M);
%Digital LPF
h = fir1(20, 0.1);
x = conv(x, h);
x = x(11:M+10);
ts = 0.001; % sampling interval
t = (0 : M-1) * ts;
% ECG signal
plot(t, x);
load ho.txt % Low pass filter
load go.txt % High pass filter
h = ho(end:-1:1);
g = go(end:-1:1);
```

```
N = 3;
[C,L] = wavedec(x, N, h, g);
L = L(:).';
Indx = [0, cumsum(L(1:end-1))];
app = C(Indx(1)+1:Indx(2));
deta = C(Indx(2)+1:Indx(3));
tsa = ts * 2^(N);
fsa = fs * 2^(-N);
banda = fs/2 * 2^(-N);
Delay = 14;
app = app(Delay + 1:end);
deta = deta(Delay + 1:end);
La = length(app);
ta = (0 : La - 1) * tsa;
% eliminating 1/3 of the lowest part of apps
appsort=sort(app);
lapp=length(appsort);
appsort=appsort(1/3*lapp:end);
th=mean(abs(appsort));
%calculating the new threshold level by feedback
appn=find(app>th);
app2=app(appn);
appsort=sort(app2);
lapp=length(appsort);
appsort=appsort(1/3*lapp:end);
th=mean(abs(appsort));
clear x app deta C L
x=ecg;
[C,L] = wavedec(x, N, h, g);
L = L(:).';
Indx = [0, cumsum(L(1:end-1))];
```

```
app = C(Indx(1)+1:Indx(2));
deta = C(Indx(2)+1:Indx(3));
tsa = ts * 2^(N);
fsa = fs * 2^(-N);
banda = fs/2 * 2^(-N);
Delay = 14;
app = app(Delay + 1:end);
deta = deta(Delay + 1:end);
La = length(app);
ta = (0 : La - 1) * tsa;
% c is the class
c=app>th;
q=find(c==1);%qrs
M=length(x);
ts = 0.001; % sampling interval
t = (0 : M-1) * ts;
k=(q)*2^N;
figure(3);title('QRS DETECTION BEFORE POST PROCESSING')
subplot(2,1,1);plot(t, x, t(k), x(k), 'o')

%POST-PROCESSING
qn = pprocess(x, q, N)
k=qn*2^N;%time index
n = length(x);
t = (0 : n-1) * ts;
%figure(4); title('POST PROCESSING')
subplot(2,1,2);plot(t, x, t(k), x(k), 'o')
```